


RESEARCH

Open Access



YY-1224, a terpene trilactone-strengthened *Ginkgo biloba*, attenuates neurodegenerative changes induced by β -amyloid (1-42) or double transgenic overexpression of APP and PS1 via inhibition of cyclooxygenase-2

Zheng-Yi Li^{1†}, Yoon Hee Chung^{2†}, Eun-Joo Shin^{1*}, Duy-Khanh Dang¹, Ji Hoon Jeong³, Sung Kwon Ko⁴, Seung-Yeol Nah⁵, Tae Gon Baik⁶, Jin Hyeong Jhoo⁷, Wei-Yi Ong⁸, Toshitaka Nabeshima⁹ and Hyoung-Chun Kim^{1*} 

Abstract

Background: *Ginkgo biloba* has been reported to possess free radical-scavenging antioxidant activity and anti-inflammatory properties. In our pilot study, YY-1224, a terpene trilactone-strengthened extract of *G. biloba*, showed anti-inflammatory, neurotrophic, and antioxidant effects.

Results: We investigated the pharmacological potential of YY-1224 in β -amyloid (A β) (1-42)-induced memory impairment using cyclooxygenase-2 (COX-2) knockout (−/−) and APPswe/PS1dE9 transgenic (APP/PS1 Tg) mice. Repeated treatment with YY-1224 significantly attenuated A β (1-42)-induced memory impairment in COX-2 (+/+) mice, but not in COX-2 (−/−) mice. YY-1224 significantly attenuated A β (1-42)-induced upregulation of platelet-activating factor (PAF) receptor gene expression, reactive oxygen species, and pro-inflammatory factors. In addition, YY-1224 significantly inhibited A β (1-42)-induced downregulation of PAF-acetylhydrolase-1 (PAF-AH-1) and peroxisome proliferator-activated receptor γ (PPAR γ) gene expression. These changes were more pronounced in COX-2 (+/+) mice than in COX-2 (−/−) mice. YY-1224 significantly attenuated learning impairment, A β deposition, and pro-inflammatory microglial activation in APP/PS1 Tg mice, whereas it significantly enhanced PAF-AH and PPAR γ expression. A preferential COX-2 inhibitor, meloxicam, did not affect the pharmacological activity by YY-1224, suggesting that the COX-2 gene is a critical mediator of the neuroprotective effects of YY-1224. The protective activity of YY-1224 appeared to be more efficacious than a standard *G. biloba* extract (Gb) against A β insult.

Conclusions: Our results suggest that the protective effects of YY-1224 against A β toxicity may be associated with its PAF antagonistic- and PPAR γ agonistic-potential as well as inhibition of the A β -mediated pro-inflammatory switch of microglia phenotypes through suppression of COX-2 expression.

Keywords: Terpene trilactone-strengthened *G. biloba*, Platelet-activating factor, Peroxisome proliferators-activated receptor γ , Microglia, APPswe/PS1dE9 transgenic mice, Cyclooxygenase-2 knockout mice

* Correspondence: shinej@kangwon.ac.kr; kimhc@kangwon.ac.kr

†Equal contributors

¹Neuropsychopharmacology and Toxicology Program, College of Pharmacy, Kangwon National University, Chuncheon 24341, Republic of Korea
Full list of author information is available at the end of the article



Background

Alzheimer's disease (AD) is the most common neurodegenerative disorder in the elderly and is associated with progressive memory loss and cognitive dysfunction [1–4]. Although the precise cause of the AD is unknown, β -amyloid peptide ($A\beta$)-induced neurotoxicity, tau pathology, and neuroinflammatory responses by microglia are thought to contribute to the pathogenesis of AD [1, 5]. Several studies have suggested that treatment with nonsteroidal anti-inflammatory drugs (NSAIDs) attenuates the loss of cognitive function and decreases the risk of developing AD [6, 7]. NSAIDs act by inhibiting cyclooxygenase (COX), which is the rate-limiting enzyme for the conversion of arachidonic acid into inflammatory mediators, which include prostaglandin E2 (PGE2). COX-2 enzymatically mediates the inflammatory response, and its expression is significantly increased in the AD brain [8, 9].

Platelet-activating factor (PAF) is a highly potent inflammatory mediator and a potential neurotoxin [10]. It plays an important role in excitotoxicity, production of free radicals and nitric oxide (NO), and regulation of pro-inflammatory cytokine genes [11–14]. The biological action of PAF is mostly mediated by binding to its G protein-coupled membrane-associated receptor (PAFR) [15]. In vitro studies have shown that activation of epidermal PAFR results in biosynthesis of COX-2 [16]. Both PAFR and COX-2 are involved in memory processing in vivo [17, 18]. PAF is a short-lived molecule due to its rapid degradation by PAF acetylhydrolase (PAF-AH; EC 3.1.1.47) [19]. PAF-AH is an enzyme that hydrolyzes an acetyl ester at the sn-2 position of PAF, converting it into its inactive metabolite, 1-O-alkyl-sn-glycero-3-phosphocholine (lysoPAF) [20]. Three isoforms of PAF-AH were identified: plasma PAF-AH and PAF-AH II and I [21].

NSAIDs may regulate gene expression via their interaction with peroxisome proliferators-activated receptors (PPARs). There are three PPAR isoforms: PPAR α , β , and γ . PPAR γ , in particular, has been implicated in inflammation and neurodegeneration [22]. The messenger RNA (mRNA) levels of PPAR γ are increased in AD patients [23], suggesting that PPAR γ may play an important role in modulating the pathophysiology of AD. The PPAR γ isoform can be activated by NSAIDs, and its activation in the microglia suppressed the expressions of inflammatory cytokines, inducible NO synthase (iNOS), and COX-2 [24]. $A\beta$ -induced activation of microglia was suppressed by a PPAR γ agonist in vitro [24]. Furthermore, PPAR γ agonists significantly decreased $A\beta_{42}$ levels in vivo [25].

It has been demonstrated that a standardized *G. biloba* extract (Gb) contains flavonoids and terpene trilactones, and possesses free radical-scavenging and antioxidant activities [26, 27]. Gb is commonly consumed as a dietary supplement for many disorders of the central nervous system (CNS), such as memory impairment, AD, and multi-

infarct dementia [28–31]. Gb has been shown to protect against $A\beta$ -induced neurotoxicity [32, 33]. In addition, Gb showed anti-inflammatory activity through the antagonism of PAF [34, 35]. Among the constituents of terpene trilactones, ginkgolides A, B, and C are highly selective and competitive PAFR antagonists [33].

The novel extract of *G. biloba*, YY-1224, consists of 24% flavonoids and 12% terpene trilactones (ginkgolides A, B, and C and bilobalide) (Table 1 and Additional file 1: Figure S1). Given that Gb generally contains 22–27% flavonoid glycosides and 5–7% terpene lactones, increased terpenoid levels are likely to be responsible for the protective activity of YY-1224 [36]. Bilobalide and ginkgolide B have neuroprotective activity [37–42]. Pilot studies indicated that YY-1224 had significant neurotrophic and antioxidant activities (Additional file 1: Figures S3 and S4). In addition, YY-1224 inhibited the COX-2 mRNA or protein expression induced by $A\beta$ (1-42) in mouse hippocampus, PC12 cells, or mixed cortical cells (Additional file 1: Figure S5). Furthermore, YY-1224 attenuated $A\beta$ (1-42)-induced cell death in PC12 cells or mixed cortical cells (Additional file 1: Figure S6). We used COX-2 knockout (–/–) mice and APP^{swe}/PS1^{dE9} transgenic (APP/PS1 Tg) mice to examine whether YY-1224 affects $A\beta$ (1-42)-induced learning impairment and inflammatory responses when compared with Gb. Our results suggest that treatment with YY-1224 significantly attenuates $A\beta$ (1-42)-induced memory impairments and pro-inflammatory responses via COX-2 suppression by inhibiting PAF and activating PPAR γ . In addition, the prolonged treatment with YY-1224 enhances memory function and decreases $A\beta$ peptide deposits and pro-inflammatory microglial activation in APP/PS1 Tg mice via COX-2 inhibition.

Methods

Animals and drug treatment

The present study was performed in accordance with the Institute for Laboratory Research (ILAR) Guidelines for the Care and Use of Laboratory Animals. COX-2 (–/–)- and COX-2 (+/+)- mice were described previously [43, 44]. Breeding pairs of double transgenic mice expressing

Table 1 Contents of Gb and YY-1224

Contents		Gb (%)	YY-1224 (%)
Ginkgo flavone glycosides	Quercetin	24	24.6
	Kaempferol		
	Isorhamnetin		
Terpene trilactones	Bilobalide	6	12.9
	Ginkgolide A		
	Ginkgolide B		
	Ginkgolide C		

Swedish mutant amyloid precursor protein gene and mutant presenilin-1 (deletion of exon 9) gene [APP^{swe}/PSEN1^{dE9} double Tg mice; B6C3-Tg (APP^{swe}, PSEN1^{dE9}) 85Dbo/J, The Jackson Laboratory, Bar Harbor, ME, USA] were bred and housed in an approved animal facility at Kangwon National University. Animals were maintained on a 12/12-h light/dark cycle and fed ad libitum and were adapted to these conditions for 2 weeks before the experiment.

A β (1-42) and A β (42-1) were purchased from American Peptide (Sunnyvale, CA, USA). A β (1-42) and A β (42-1) were dissolved in 0.1 M PBS at pH 7.4, and aliquots were stored at -20 °C. A β peptides in each aliquot were aggregated by incubation in sterile distilled water at 37 °C for 4 days. Six-month-old COX-2 (-/-)- and COX-2 (+/+)-mice were administered A β (1-42) and A β (42-1) (400 pmol, i.c.v. injection) according to the procedure established by Laursen and Belknap [45]. Each mouse was injected in the bregma using a 10- μ l microsyringe (Hamilton, Reno, NV, USA) fitted with a 26-gauge needle inserted at a depth of 2.4 mm. The injection volume was 5 μ l. The injection placement and needle track were visible and could be verified during dissection.

YY-1224 and a standard *G. biloba* extract (Gb) were obtained from the research center of Yuyu Pharma Inc. (Suwon, Republic of Korea). The content and representative HPLC chromatogram of each component in YY-1224 or Gb are shown in Table 1 and Additional file 1: Figure S1, respectively. YY-1224 (50 mg/kg) or Gb (50 mg/kg) was dissolved in 10% tween-80 and administered orally in a volume of 1 ml/kg. YY-1224 or Gb administration began 7 days before the A β i.c.v. injection, and the drug administration was continued once a day throughout the experimental period. The behavioral study commenced on day 3 after A β i.c.v. injection and was carried out sequentially. During the behavioral study, YY-1224 or Gb was administered 30 min after the behavioral test to avoid a direct effect on performance. The experimental design is shown in Fig. 1a and Additional file 1: Figure S2.

In addition, 6-month-old APP^{swe}/PS1^{dE9} double Tg mice were treated with YY-1224 (50 mg/kg, p.o.) or Gb (50 mg/kg, p.o.) with or without the preferential COX-2 inhibitor, meloxicam (10 mg/kg, p.o.; Sigma-Aldrich, St. Louis, MO, USA), once a day for 3 months. Meloxicam was suspended in 0.5% sodium carboxymethyl cellulose (Na-CMC) immediately before use. The behavioral study was started when the mice were 9 months old, and additional treatment with YY-1224, Gb, or meloxicam was continued during the behavioral study. During the behavioral study, drugs were administered 30 min after the behavioral test to avoid a direct effect on performance. The experimental design is shown in Fig. 1b.

Y-maze test

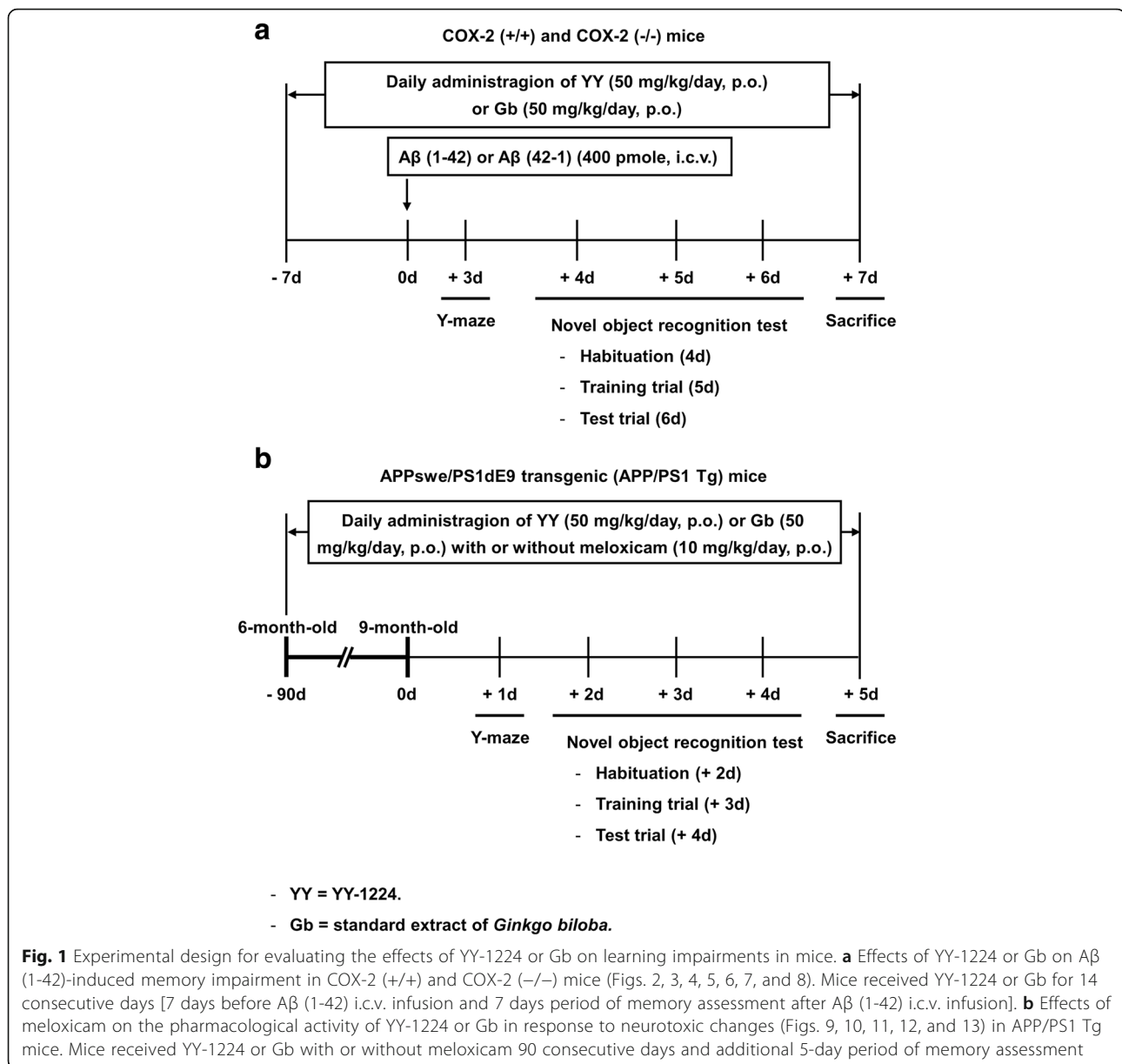
The Y-maze test was performed as described previously [46]. Briefly, the Y-shaped maze was constructed of black acrylic with three identical arms separated by 120°. Each arm was 40 cm long, 12 cm tall, and 10 cm wide. The mouse was placed at the end of one arm and allowed to move freely through the maze during an 8-min session. The percent alternation was calculated as the ratio of actual to possible alternations (defined as the total number of arm entries minus two) multiplied by 100.

Novel object recognition test

The novel object recognition test was performed as described previously [47, 48]. On the training trial, two different objects were fixed on the floor in a symmetric position from the center of the open field box (40 \times 40 \times 35 high cm), 20 cm from each other and 10 cm from the nearest wall, and each mouse was allowed to explore the objects for 10 min. Mice were subjected to the test trial 24 h after the training trial. One of the familiar objects used during training trial was replaced by a novel object, and each mouse was then allowed to explore the objects for 10 min. Time spent exploring each object was recorded and analyzed with a video tracking system (EthoVision, Noldus, The Netherlands). Novel object recognition was expressed as a “recognition index (%)” the percentage of time spent exploring the novel object over the total time spent exploring both objects.

Immunocytochemistry

Immunocytochemistry and staining quantification were performed as described previously [46, 49, 50]. Mice were perfused transcardially with 50 mL of ice-cold PBS (10 mL/10 g body weight) followed by 4% paraformaldehyde (20 mL/10 g body weight). Brains were removed and stored in 4% paraformaldehyde overnight. The brains were cut on a horizontal sliding microtome into 35- μ m transverse free-floating sections. Every sixth section of the dorsal hippocampus (total of four sections) from each brain was collected for immunocytochemistry. Sections were blocked with PBS containing 0.3% hydrogen peroxide for 30 min and then incubated in PBS containing 0.4% Triton X-100 and 1% normal serum for 20 min. Antigen retrieval with formic acid (70%, 10 min) was performed to detect A β deposition in APP^{swe}/PS1^{dE9} double Tg mice. After a 48-h incubation with primary antibody against PAFR (1:200; Cayman Chemical, Ann Arbor, MI, USA), PAF-AH (1:80; Santa Cruz Biotechnology, Inc., Santa Cruz, CA, USA), A β (1:50; Invitrogen, Thermo Fisher Scientific, Camarillo, CA, USA), or Iba-1 (1:500, Wako Pure Chemical Industries, Chuo-ku, Osaka, Japan), sections were incubated with the biotinylated secondary antibody (1:1000; Vector Laboratories, Burlingame, CA, USA) for 1 h. The sections were then immersed in a solution containing avidin–biotin peroxidase



complex (Vector Laboratories) for 1 h, and 3,3'-diaminobenzidine was utilized as the chromogen. Digital images were acquired at $\times 4$, $\times 10$, or $\times 20$ objective magnification using an Olympus microscope (BX51; Olympus) and a digital microscope camera (DP72; Olympus). ImageJ version 1.47 software (National Institutes of Health, Bethesda, MD, USA) was employed to quantify images. Briefly, images were converted to 8-bit grayscale images and were subjected to background subtraction to correct for uneven background. To measure PAFR- or PAF-AH-immunoreactivity, the pyramidal cell layer of CA1 and CA3 regions from each section were selected as the region of interest (ROI). Threshold values were set to select the immunoreactive area. The integrated density of

each ROI was measured, and the value was expressed as density per micrometer square. For staining quantification of A β or Iba-1, the entire hippocampus and the cortical area containing primary somatosensory cortex were selected as the ROIs. Threshold values were set to identify immunoreactive areas, and particle analysis was employed to measure the area fraction of A β - or Iba-1-immunoreactivity (Additional file 1: Figure S13).

Western blot

Tissues were lysed in buffer containing a 200-mM Tris-HCl (pH 6.8), 1% SDS, 5 mM EGTA, 5 mM EDTA, 10% glycerol, 1 \times phosphatase inhibitor cocktail I (Sigma-Aldrich), and 1 \times protease inhibitor cocktail (Sigma-Aldrich).

The lysate was centrifuged at $12,000 \times g$ for 30 min, and the supernatant fraction was used for Western blot analysis as described previously [48–50]. Proteins (20 $\mu\text{g}/\text{lane}$) were separated by 8 or 10% sodium dodecyl sulfate-polyacrylamide gel electrophoresis (PAGE) and transferred onto polyvinylidene fluoride (PVDF) membranes. Following transfer, the membranes were preincubated with 5% non-fat milk for 30 min and incubated overnight at 4 °C with primary antibody against PPAR- γ (1:200; Santa Cruz Biotechnology, Inc.) or β -actin (1:50000; Sigma-Aldrich). Membranes were then incubated with HRP-conjugated secondary anti-rabbit IgG (1:1000, GE Healthcare, Piscataway, NJ, USA) or anti-mouse IgG (1:1000, Sigma-Aldrich) for 2 h. Subsequent visualization was performed using an enhanced chemiluminescence system (ECL plus[®], GE Healthcare). Relative intensities of the bands were quantified with PhotoCapt MW (version 10.01 for Windows; Vilber Lourmat, Marne la Vallée, France), and then normalized to the intensity of β -actin.

Reverse transcription and real-time polymerase chain reaction (RT-rt-PCR)

Reverse transcription and real-time polymerase chain reaction (RT-rt-PCR) was performed as described previously [51]. Total RNA was isolated from the hippocampus using an RNeasy Mini Kit (Qiagen, Valencia, CA, USA) according to the manufacturer's instructions. Reverse transcription reactions were carried out using the RNA to cDNA EcoDry Premix (Clontech, Palo Alto, CA, USA) with a 1-h incubation at 42 °C. For rt-PCR, 0.5 μL of complementary DNA (cDNA) was added to 50 μL of total PCR reaction mixture, containing 25 pmol of each primer and QuantiTect SYBR Green PCR Master Mix (Qiagen). rt-PCR was performed using a CFX96 Touch real-time PCR system (Bio-Rad Laboratories, Hercules, CA, USA). The reference gene (GAPDH) and target gene from each sample were run in parallel in the same plate with the same amount of cDNA. Primer sequences are listed in Table 2. After activation of HotStarTaq DNA polymerase at 95 °C for 15 min, PCR was performed as 40 cycles of denaturation at 94 °C for 1 min, annealing at 60 °C for 1 min, and extension at 72 °C for 1 min. The relative mRNA expression level was normalized to that of GAPDH ($2^{\text{Ct}(\text{GAPDH}) - \text{Ct}(\text{each gene})}$).

Determination of malondialdehyde

The amount of lipid peroxidation in the hippocampus was determined by measuring the level of thiobarbituric acid-reactive substance in homogenates and is expressed in terms of malondialdehyde (MDA) content. The MDA level was measured using HPLC-UV/VIS detection system (model LC-20AT and SPD-20A, Shimadzu, Kyoto, Japan) as described by Richard et al. [52] with slight modifications [49, 53]. Briefly, each hippocampal tissue was homogenized in PBS, and 0.1 ml of this homogenate

(or standard solutions prepared daily from 1,1,3,3-tetramethoxypropane) and 0.75 ml of the working solution (thiobarbituric acid 0.37% and perchloric acid 6.4%, 2:1, *v:v*) were mixed and heated to 95 °C for 1 h. After cooling (10 min in ice water bath), the flocculent precipitate was removed by centrifugation at $3200 \times g$ for 10 min. The supernatant was neutralized and filtered prior to injection. Isocratic separation was achieved on a 5- μm ODS column with mobile phase consisting of 50 mM PBS (pH 6.0): methanol (58:42, *v/v*) at a flow rate of 1.0 mL/min. The effluents were monitored at 532 nm.

Determination of protein carbonyls

The extent of protein oxidation in the hippocampus was assessed by measuring the content of protein carbonyl groups, which was determined spectrophotometrically with the 2,4-dinitrophenylhydrazine (DNPH)-labeling procedure, as described by Oliver et al. [54]. Results are expressed as nanomoles of DNPH incorporated/mg protein [49, 53] based on the extinction coefficient for aliphatic hydrazones at $21 \text{ mM}^{-1} \cdot \text{cm}^{-1}$.

Determination of synaptosomal reactive oxygen species (ROS) formation

Synaptosomal fractions were obtained as described by Whittaker et al. [55], with minor modifications [49, 53]. The protein concentration of the synaptosomal preparation was measured using the BCA protein assay reagent (Pierce, Rockford, IL, USA) and was found to be approximately 5 mg of protein per milliliter. ROS formation was assessed by measuring the conversion from 2',7'-dichlorofluorescein diacetate (DCFH-DA) to dichlorofluorescein (DCF) as described by Lebel and Bondy [56]. Briefly, hippocampal synaptosomes were incubated with 5 μM DCFH-DA (Molecular Probes, Eugene, OR, USA) for 15 min at 37 °C. Excess unbound probe was removed by centrifugation at $12,500 \times g$ for 10 min. The fluorescence intensity due to ROS was measured at an excitation wavelength of 488 nm and an emission wavelength of 528 nm. DCF (Sigma-Aldrich) was used as a standard.

Determination of 4-hydroxy-2-nonenal (4-HNE) and protein carbonyl by slot blot analysis

Determination of 4-HNE was performed using slot blot analysis as described previously [49]. Following adsorption, the PVDF membranes were preincubated with 5% non-fat milk and incubated overnight at 4 °C with anti-4-HNE antibody (1:2000, Calbiochem, La Jolla, CA, USA). After incubation with the primary antibody, membranes were incubated with a HRP-conjugated secondary antibody. Subsequent visualization was performed using an enhanced chemiluminescence system (ECL plus[®], GE

Table 2 Gene primer sequences for RT-rt-PCR analysis

Gene	Primer sequences (5'-3')	Expected size (bp)	Gene bank accession number
PAFR	F: CAACGAGGGCGACTGGATT R: GACACCCAAAAAGGCCACACT	97	D50872.1 [93]
PAF-AH I α 1	F: ACACAGCATGTA CTCTGGCG R: GCATCTAAGAAGTGGGCTCG	293	BC067015.1 [93]
PAF-AH I α 2	F: AGAATGCCAAGGTGAACCG R: AAATCAAACATGTCGTGCCA	127	BC056211.2 [94]
PAF-AH I LIS1	F: GATGACAAGACCCTCCGTGT R: GAGCTCAAATGGGGTAACCA	240	NM_013625.4 [95]
PAF-AH II	F: ATCAAGGAAGGGGAGAAGGA R: AAGGAGTGACCCATCACGGC	200	BC021890.1 [96]
TNF- α	F: CATCTTCTCAAAATTCGAGTGACAA R: TGGGAGTAGACAAGGTACAACCC	175	D84199.2 [97]
IL-1 β	F: GAAAGACGGCACCCACC R: AGACAAACCGCTTTTCCATCTTC	83	BC011437.1 [98]
IL-6	F: TGGAGTCACAGAAGGAGTGGCTAAG R: TCTGACCACAGTGAGGAATGTCCAG	155	BC132458.1
INF- γ	F: TCAAGTGGCATAGATGTGGAAGAA R: TGGCTCTGCAGGATTTTCATG	92	BC119063.1 [97]
iNOS	F: CAGCTGGGCTGTACAAACCTT R: CATTGGAAGTGAAGCGTTTCG	95	BC062378.1 [97]
PPAR- α	F: CCCTGAACATCGAGTGTCCGAA R: TTGCAGCTCCGATCACACTT	142	BC016892.1 [99]
PPAR- γ	F: TGTGCGTTTCAGAAAGTGCCTT R: GCTCGCAGATCAGCAGACTCT	146	AB644275.1
YM1	F: ACCCCTGCCTGTGTA CTACCT R: CACTGAACGGGGCAGGTCCAAA	183	BC061154.1 [100]
CD206	F: TCTTTGCCTTTCCAGTCTCC R: TGACACCCAGCGGAATTC	241	NM_008625.2 [101]
CD16	F: TTTGGACACCCAGATGTTTCAG R: GTCTTCTTGAGCACCTGGATC	163	NM_010188.5 [101]
CD32	F: AATCCTGCCGTTCTACTGATC R: GTGTCACCGTGTCTTCTTGAG	187	BC038070.1 [101]
CD86	F: TTGTGTGTGTTCTGAAACGGAG R: AACTTAGAGGCTGTGTTGCTGGG	202	BC013807.1 [101]
COX-2	F: CCACTTCAAGGGAGTCTGGA R: AGTCATCTGCTACGGGAGGA	197	NM_011198.3 [102]
GAPDH	F: GCCAAGGCTGTGGCAAGGT R: TCTCCAGGCGGCACGTCAGA	112	GU214026.1 [103]

Healthcare). The amount of oxidized proteins was measured using the Oxyblot kit [Chemicon (EMD Millipore), Temecula, MA, USA] according to the instructions provided by the manufacturer. Briefly, the protein carbonyl content was labeled with protein hydrazone derivatives using 2,4-dinitrophenylhydrazide (DNP). Each blot was

preincubated with 5% non-fat milk and then incubated with the primary antibody (1:100) specific to the DNP moiety, followed by incubation with a HRP-conjugated secondary antibody. Subsequent visualization was performed using an enhanced chemiluminescence system (ECL plus[®], GE Healthcare) [49].

Statistics

Data were analyzed using IBM SPSS ver. 21.0 (IBM, Chicago, IL, USA). Analysis of variance (ANOVA) was employed for the statistical analysis of the effect of Aβ treatment, pretreatment (YY-1224 or Gb), or COX-2 inhibition (COX-2 gene knockout or COX-2 inhibitor). Post hoc Fisher's least significant difference pairwise comparisons tests were then conducted. *P* values <0.05 were considered to be significant.

Results

Effect of YY-1224 or Gb on Aβ (1-42)-induced impairment of visual recognition learning in COX-2 (+/+)- and COX-2 (-/-)-mice

The recognition test is based on the natural tendency of rodents to investigate a novel object instead of a familiar one. The choice to explore the novel object reflects the use of learning and (recognition) memory processes. There was no significant difference between Aβ-treated groups in exploratory preference for objects in the training trial. The exploratory preference for a novel object was significantly decreased [Fig. 2a, ANOVA and post hoc pairwise comparisons showing the effect of Aβ (1-42), *P* < 0.01] in Aβ (1-42)-treated mice when compared

with Aβ (42-1)-treated mice. In the COX-2 (+/+) mice, repeated treatment with Gb or YY-1224 significantly ameliorated the decrease in exploratory preference for a novel object that was induced by Aβ (1-42) [Fig. 2a, ANOVA and post hoc pairwise comparisons indicating the effect of Gb (*P* < 0.05) or YY-1224 (*P* < 0.01)]. Genetic depletion of COX-2 also significantly attenuated the Aβ (1-42)-induced decrease in the exploratory preference for a novel object (Fig. 2a, ANOVA and post hoc pairwise comparisons showing the effect of COX-2 gene knockout, *P* < 0.05), and YY-1224 or Gb did not provide additional cognitive enhancing effects in COX-2 (-/-) mice.

Effects of YY-1224 or Gb on Aβ (1-42)-induced impairment of spatial working memory in COX-2 (+/+)- and COX-2 (-/-)-mice

The Y-maze test is based on the natural navigation behaviors of rodents and is used to evaluate spatial working memory, which is known to be dependent on hippocampal function. There was no significant change in the performance of the Y maze task between Aβ (42-1)-treated groups. In the COX-2 (+/+) mice, alternation behavior was significantly decreased [Fig. 2b, ANOVA

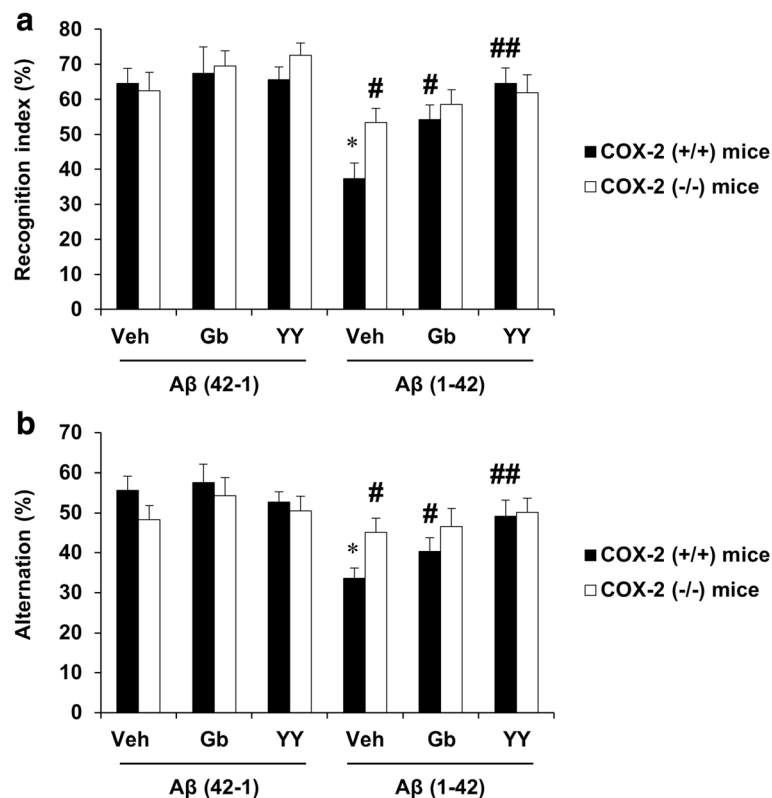


Fig. 2 Effects of YY-1224 (YY) or Gb on Aβ (1-42)-induced memory impairment in mice. **a** Novel object recognition test. **b** Y-maze test. Veh vehicle for YY or Gb (10% tween-80 in sterile saline). Each value is the mean ± S.E.M of six animals. **P* < 0.01 vs. COX-2 (+/+) mice treated with vehicle + Aβ (42-1); #*P* < 0.05, ##*P* < 0.01 vs. COX-2 (+/+) mice treated with vehicle + Aβ (1-42) (three-way ANOVA was followed by Fisher's LSD pairwise comparisons)

and post hoc pairwise comparisons showing the effect of Aβ (1-42), $P < 0.01$] in Aβ (1-42)-treated mice compared to Aβ (42-1)-treated mice. ANOVA and post hoc pairwise comparisons revealed that the Aβ (1-42)-induced decrease in alternation behavior was significantly attenuated by YY-1224 (Fig. 2b, $P < 0.01$), Gb (Fig. 2b, $P < 0.05$), or genetic inhibition of COX-2 (Fig. 2b, $P < 0.05$). YY-1224-mediated attenuation appeared to be more pronounced than Gb in COX-2 (+/+) mice; however, YY-1224 and Gb did not affect the Y-maze performance in Aβ (1-42)-treated COX-2 (-/-) mice. The results from the Morris water maze are comparable to those from the novel object recognition test and the Y-maze test (Additional file 1: Figure S7).

Effects of YY-1224 or Gb on Aβ (1-42)-induced changes in the expressions of PAFR and PAF-AH in the hippocampi of COX-2 (+/+)- and COX-2 (-/-)-mice

To explore whether PAF modulatory actions were involved in the pharmacological effect of YY-1224 against Aβ (1-42)-induced memory impairments, the expressions of PAFR and PAF-AH were examined in the hippocampus of COX-2 (+/+)- and COX-2 (-/-)-mice using immunocytochemistry and RT-rt-PCR. ANOVA and post hoc pairwise comparisons indicated that Aβ (1-42) infusion significantly increased PAFR-immunoreactivity (Fig. 3a, $P < 0.01$ for CA1 or CA3) and PAFR mRNA levels (Fig. 3b, $P < 0.01$) in the hippocampi of COX-2 (+/+) mice. Aβ (1-42)-induced increases in PAFR-immunoreactivity

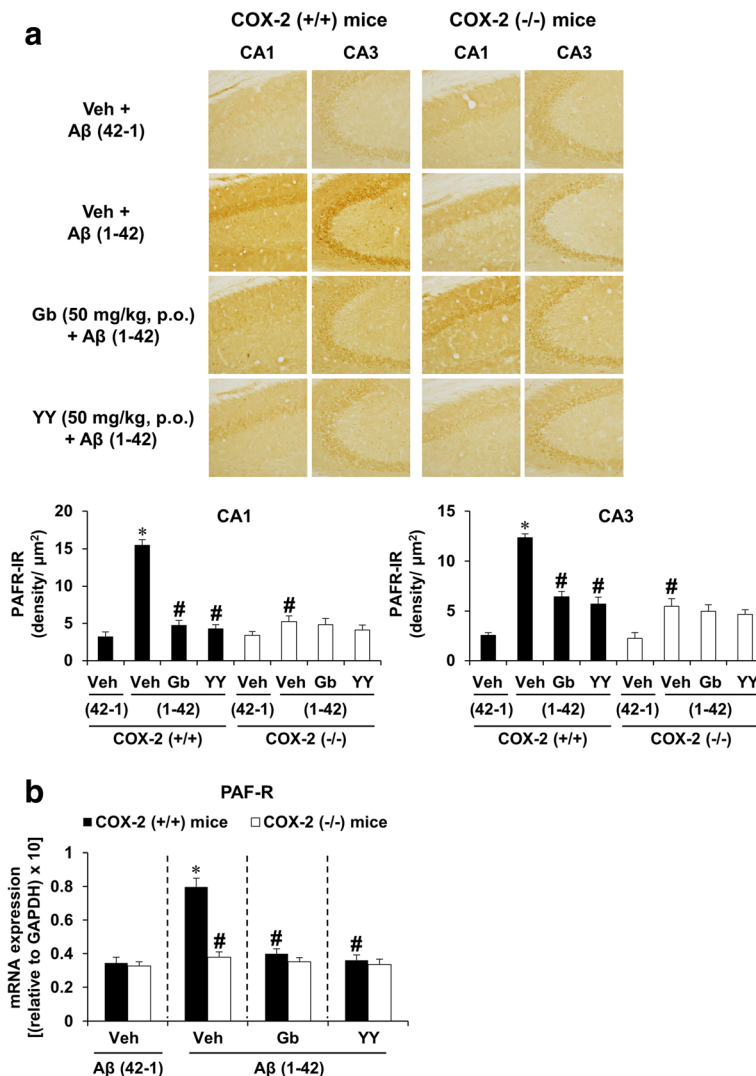


Fig. 3 Effects of YY-1224 (YY) or Gb on Aβ (1-42)-induced PAFR expression in the hippocampi of mice. **a** Effect of YY on PAFR-immunoreactivity. **b** Effect of YY on PAFR mRNA expression. Veh vehicle for YY or Gb (10% tween-80 in sterile saline). Each value is the mean ± S.E.M of six animals. * $P < 0.01$ vs. COX-2 (+/+) mice treated with vehicle + Aβ (42-1); # $P < 0.01$ vs. COX-2 (+/+) mice treated with vehicle + Aβ (1-42) (three-way ANOVA was followed by Fisher's LSD pairwise comparisons)

and PAFR mRNA expression were significantly attenuated by Gb, YY-1224, or COX-2 gene knockout (Fig. 3a, b, ANOVA and post hoc pairwise comparisons showing the effect of Gb, YY-1224, or COX-2 gene knockout, $P < 0.01$). In addition, YY-1224 and Gb did not show additional effects compared to COX-2 gene depletion (Fig. 3). The results from RT-rt-PCR of PAFR mRNA are comparable to those from RT-PCR (Additional file 1: Figure S8a).

In contrast, total PAF-AH I-immunoreactivity was significantly decreased by A β (1-42) in the hippocampi of COX-2 (+/+) mice [Fig. 4, ANOVA and post hoc pairwise comparisons showing the effect of A β (1-42), $P < 0.01$]. To examine which subunit of PAF-AH is transcriptionally regulated by A β (1-42), we examined changes in the mRNA expression level of PAF-AH I subunits using RT-rt-PCR. A β (1-42) infusion significantly decreased the mRNA expression of the $\alpha 2$ subunit, but not the $\alpha 1$ or LIS1 subunit, in the hippocampus of COX-2 (+/+) mice [Fig. 5b, ANOVA and post hoc pairwise comparisons showing the effect of A β (1-42), $P < 0.01$]. In addition, the PAF-AH II mRNA level was significantly increased after treatment with A β (1-42) [Fig. 5d, ANOVA and post hoc pairwise comparisons showing the effect of A β (1-42), $P < 0.01$]. These changes in PAF-AH I-immunoreactivity,

PAF-AH I $\alpha 2$ mRNA expression, and PAF-AH II mRNA expression were significantly reversed by Gb, YY-1224, and COX-2 gene depletion (Fig. 5b, d, ANOVA and post hoc pairwise comparisons showing the effect of Gb, YY-1224, or COX-2 gene knockout, $P < 0.01$). YY-1224 appeared to be more effective in enhancing PAF-AH I $\alpha 2$ mRNA expression than Gb in COX-2 (+/+) mice (Fig. 5b, ANOVA and post hoc pairwise comparisons showing the difference between Gb and YY-1224, $P < 0.05$). YY-1224 and Gb did not show additional effects compared to COX-2 gene depletion in the presence of A β (1-42) (Figs. 4 and 5). The results from RT-rt-PCR of the mRNA expression of PAF-AH subtypes are comparable to those from RT-PCR (Additional file 1: Figure S8b-d).

Effects of YY-1224 or Gb on lipid peroxidation, protein oxidation, and reactive oxygen species (ROS) formation induced by A β (1-42) in the hippocampi of COX-2 (+/+) and COX-2 (-/-) mice

To evaluate whether COX-2 inhibitory action is involved in the pharmacological effect of YY-1224 against A β (1-42)-induced oxidative burdens, the level of oxidative stress markers, including lipid peroxidation, protein expression, and ROS formation was measured in the hippocampus of

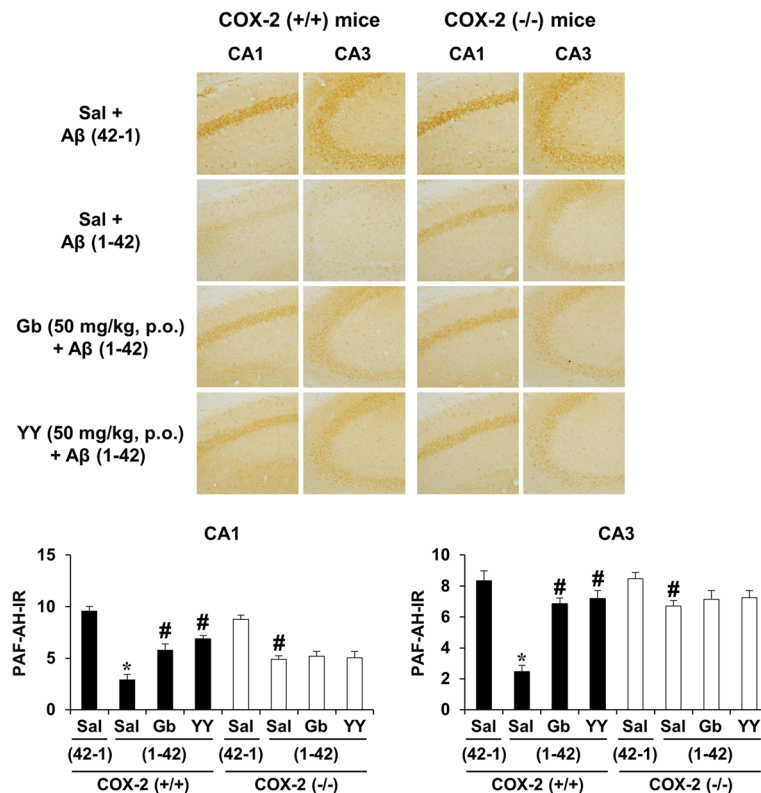


Fig. 4 Effects of YY-1224 (YY) or Gb on A β (1-42)-induced PAF-AH I-immunoreactivity in the hippocampi of mice. Veh vehicle for YY or Gb (10% tween-80 in sterile saline). Each value is the mean \pm S.E.M of six animals. * $P < 0.01$ vs. COX-2 (+/+) mice treated with vehicle + A β (42-1); # $P < 0.01$ vs. COX-2 (+/+) mice treated with vehicle + A β (1-42) (three-way ANOVA was followed by Fisher's LSD pairwise comparisons)

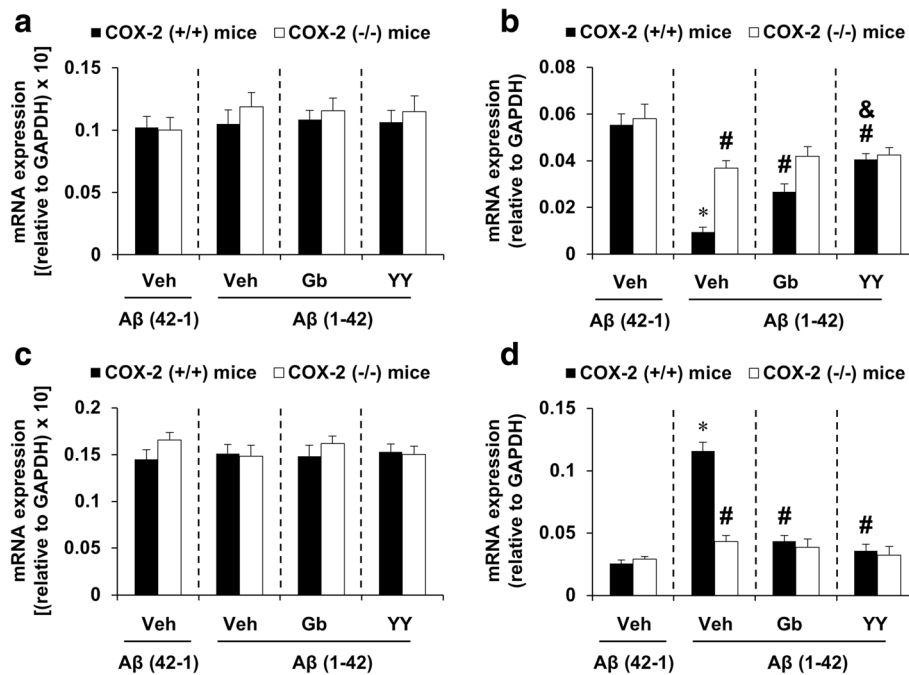


Fig. 5 Effects of YY-1224 (YY) or Gb on A β (1-42)-induced PAF-AH mRNA levels in the hippocampus. **a** Changes in PAF-AH I α 1 mRNA expression. **b** Changes in PAF-AH I α 2 mRNA expression. **c** Changes in PAF-AH I LIS1 mRNA expression. **d** Changes in PAF-AH II mRNA expression. Veh vehicle for YY or Gb (10% tween-80 in sterile saline). Each value is the mean \pm S.E.M of six animals. * $P < 0.01$ vs. COX-2 (+/+) mice treated with vehicle + A β (42-1); # $P < 0.01$ vs. COX-2 (+/+) mice treated with vehicle + A β (1-42); & $P < 0.05$ vs. COX-2 (+/+) mice treated with Gb + A β (1-42) (three-way ANOVA was followed by Fisher's LSD pairwise comparisons)

COX-2 (+/+)- and COX-2 (-/-)-mice. Treatment with A β (1-42) resulted in an increase in lipid peroxidation, as assessed by MDA and 4-HNE level, protein oxidation, as shown by protein carbonyl level and expression, and synaptosomal ROS formation in COX-2 (+/+) mice [Fig. 6, ANOVA and post hoc pairwise comparisons showing the effect of A β (1-42), $P < 0.01$]. ANOVA and post hoc pairwise comparisons indicated that YY-1224 and Gb treatment significantly attenuated A β (1-42)-induced lipid peroxidation (Fig. 6a, YY-1224 and Gb, $P < 0.01$ for MDA and 4-HNE), protein oxidation (Fig. 6b, YY-1224, $P < 0.01$ or Gb $P < 0.05$ for protein carbonyl level; YY-1224 and Gb, $P < 0.01$ for protein carbonyl expression), and synaptosomal ROS formation (Fig. 6c, YY-1224, $P < 0.01$ or Gb $P < 0.05$) in COX-2 (+/+) mice. COX-2 gene depletion also significantly attenuated oxidative stress induced by A β (1-42) (Fig. 6, ANOVA and post hoc pairwise comparisons showing the effect of COX-2 gene knockout, $P < 0.01$ for all parameters). YY-1224 attenuated A β (1-42)-induced protein oxidation and ROS formation in COX-2 (+/+) mice more effectively than Gb (Fig. 6b, c, ANOVA and post hoc pairwise comparisons showing the difference between Gb and YY-1224, $P < 0.05$), but neither showed additional effects over COX-2 gene depletion (Fig. 6).

Effects of YY-1224 or Gb on changes in the expression of pro-inflammatory cytokines [tumor necrosis factor alpha (TNF- α), interleukin-1 beta (IL-1 β), interleukin-6 (IL-6), and interferon gamma (IFN- γ)] and iNOS induced by A β (1-42) in the hippocampi of COX-2 (+/+)- and COX-2 (-/-)-mice
To understand whether COX-2 inhibitory action was involved in the pharmacological effect of YY-1224 against A β (1-42)-induced pro-inflammatory changes, the mRNA levels of pro-inflammatory markers were examined in the hippocampus of COX-2 (+/+)- and COX-2 (-/-)-mice using RT-rt-PCR. As shown in Fig. 7, the mRNA expression of TNF- α , IL-1 β , IL-6, and iNOS, but not IFN- γ , was significantly increased by A β (1-42) in COX-2 (+/+) mice [Fig. 7a-c, e, ANOVA and post hoc pairwise comparisons showing the effect of A β (1-42), $P < 0.01$]. YY-1224, Gb, and COX-2 gene depletion significantly attenuated these increases (Fig. 7a-c, e, ANOVA and post hoc pairwise comparisons showing the inhibitory effect of YY-1224, Gb, and COX-2 gene knockout, $P < 0.01$). ANOVA and post hoc pairwise comparisons showed that YY-1224 had a more pronounced effect than Gb on the increases in IL-1 β , IL-6, and iNOS induced by A β (1-42) in COX-2 (+/+) mice (Fig. 7b, c and e, $P < 0.05$ for IL-1 β and iNOS; $P < 0.01$ for IL-6). YY-1224 and Gb did not show additional effects compared to COX-2 gene depletion in the

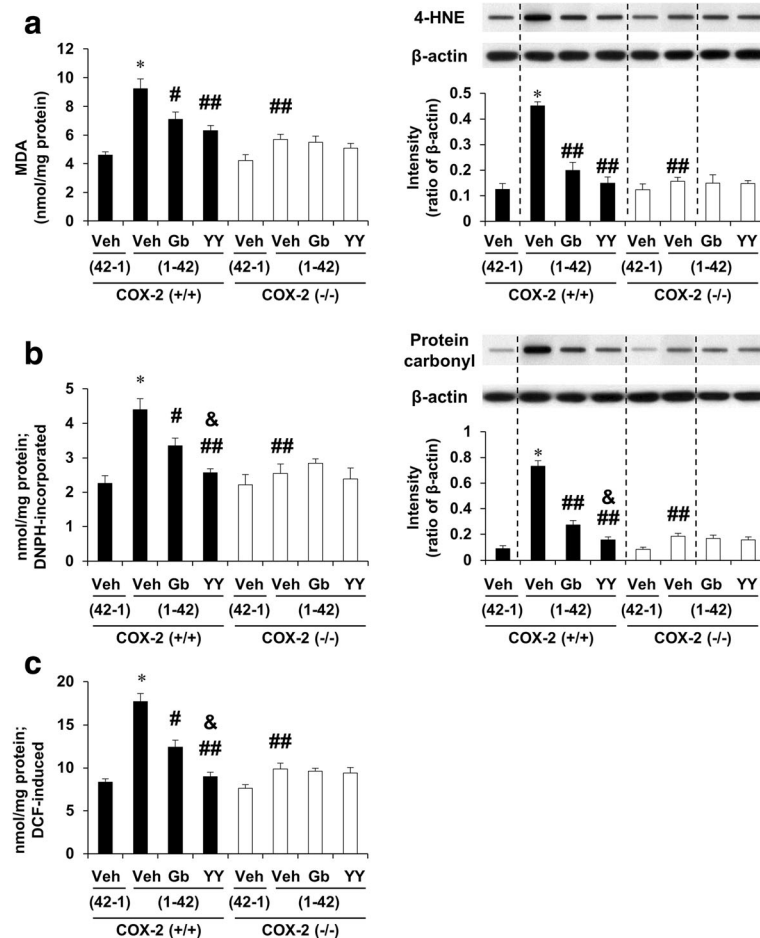


Fig. 6 Effects YY-1224 (YY) or Gb on A β (1-42)-induced oxidative burdens in the hippocampus of mice. **a** A β (1-42)-induced lipid peroxidation. **b** A β (1-42)-induced protein oxidation. Lipid peroxidation and protein oxidation were evaluated by quantitative biochemical analyses and slot blot analyses. **c** A β (1-42)-induced synaptosomal formation of reactive oxygen species. Veh vehicle for YY or Gb (10% tween-80 in sterile saline). Each value is the mean \pm S.E.M of six animals. * $P < 0.01$ vs. COX-2 (+/+) mice treated with vehicle + A β (42-1); # $P < 0.05$, ## $P < 0.01$ vs. COX-2 (+/+) mice treated with vehicle + A β (1-42); & $P < 0.05$ vs. COX-2 (+/+) mice treated with Gb + A β (1-42) (three-way ANOVA was followed by Fisher's LSD pairwise comparisons)

presence of A β (1-42) (Fig. 7). The results from RT-rt-PCR of the mRNA expression of pro-inflammatory factors were comparable to those from RT-PCR (Additional file 1: Figure S9).

Effects of YY-1224 or Gb on changes in PPAR γ expression induced by A β (1-42) in the hippocampi of COX-2 (+/+) and COX-2 (-/-) mice

As mentioned above, it has been suggested that PPAR γ is related to inflammatory and neurodegenerative processes [22]. To explore whether PPARs modulatory actions are involved in the anti-inflammatory effect of YY-1224, the mRNA or protein expression of PPAR α or PPAR γ was examined after A β (1-42) infusion in the hippocampus of COX-2 (+/+)- and COX-2 (-/-)-mice. A β (1-42) infusion significantly decreased the mRNA and protein expression

of PPAR γ in COX-2 (+/+) mice [Fig. 8b, c, ANOVA and post hoc pairwise comparisons showing the effect of A β (1-42), $P < 0.01$]. A β (1-42)-induced decreases in PPAR γ mRNA and protein expression were significantly attenuated by YY-1224, Gb, or COX-2 gene knockout (Fig. 8b, c, ANOVA and post hoc pairwise comparisons showing the inhibitory effect of YY-1224, Gb, and COX-2 gene knockout, $P < 0.01$). YY-1224 mediated significant attenuation than Gb in COX-2 (+/+) mice (Fig. 8b, c, ANOVA and post hoc pairwise comparisons showing the difference between Gb and YY-1224, $P < 0.05$). YY-1224 and Gb did not show additional effects compared to COX-2 gene depletion (Fig. 8). The results from RT-rt-PCR of the PPAR α or PPAR γ mRNA expression were comparable to those from RT-PCR (Additional file 1: Figure S10).

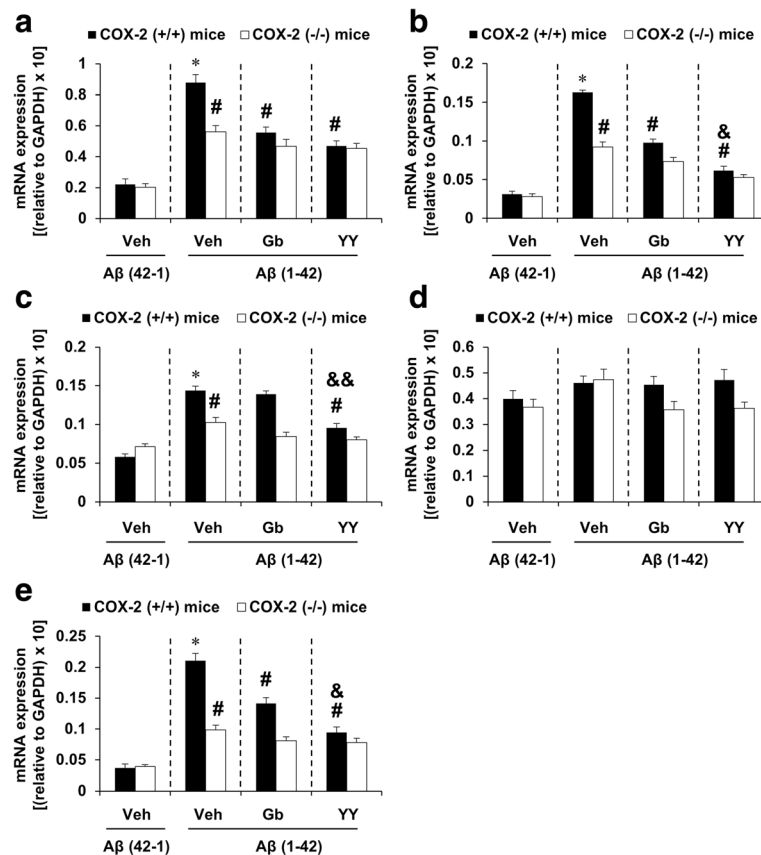


Fig. 7 Effects of YY-1224 (YY) or Gb on Aβ (1-42)-induced proinflammatory genes in the hippocampi of mice. **a** Changes in TNF-α mRNA expression. **b** Changes in IL-1β mRNA expression. **c** Changes in IL-6 mRNA expression. **d** Changes in IFN-γ mRNA expression. **e** Changes in iNOS mRNA expression. Veh vehicle for YY or Gb (10% tween-80 in sterile saline). Each value is the mean ± S.E.M of six animals. * $P < 0.01$ vs. COX-2 (+/+) mice treated with vehicle + Aβ (42-1); # $P < 0.01$ vs. COX-2 (+/+) mice treated with vehicle + Aβ (1-42); & $P < 0.05$, && $P < 0.05$ vs. COX-2 (+/+) mice treated with Gb + Aβ (1-42) (three-way ANOVA was followed by Fisher's LSD pairwise comparisons)

Effects of meloxicam, a preferential COX-2 inhibitor, on the pharmacological effect of YY-1224 on memory dysfunction and Aβ plaque deposition in APP/PS1 Tg mice

To understand the pharmacological effects of YY-1224, we examined the effect of Gb or YY-1224 on memory dysfunction and Aβ plaque deposition in APP/PS1 Tg mice. ANOVA and post hoc pairwise comparisons showed that treatment with YY-1224 or Gb significantly increased the alternation ratio in the Y-maze test (Fig. 9a, YY-1224 or Gb, $P < 0.01$ or $P < 0.05$) and the recognition index in the novel object recognition test (Fig. 9b, YY-1224 or Gb, $P < 0.01$ or $P < 0.05$). A preferential COX-2 inhibitor, meloxicam, also significantly enhanced cognitive function in the Y-maze (Fig. 9a, $P < 0.01$) and novel object recognition tests (Fig. 9b, $P < 0.01$). Consistent with results obtained from Aβ-treated mice, YY-1224 was more effective at enhancing novel object recognition in APP/PS1 Tg mice (Fig. 9b, ANOVA and post hoc pairwise comparisons showing the difference between Gb and YY-1224, $P < 0.05$), and meloxicam treatment did not

affect the performance of YY-1224- or Gb-treated APP/PS1 Tg mice (Fig. 9a, b).

YY-1224, Gb, or meloxicam treatment significantly attenuated Aβ plaque deposition in the hippocampus and cortex of APP/PS1 Tg mice (Fig. 9c, d, ANOVA and post hoc pairwise comparisons showing the inhibitory effect of YY-1224, Gb, and meloxicam, $P < 0.01$ for hippocampus and cortex). Attenuation mediated by YY-1224 was more pronounced than attenuation mediated by Gb (Fig. 9c, d, ANOVA and post hoc pairwise comparisons showing the difference between Gb and YY-1224, $P < 0.05$ for hippocampus and cortex). Meloxicam did not affect responses to pharmacological activity in YY-1224- or Gb-treated APP/PS1 Tg mice (Fig. 9c, d).

Effects of meloxicam on pharmacological activity mediated by YY-1224 through PAF-AH I and PPARγ expression in the hippocampi of APP/PS1 Tg mice

Because YY-1224 exerted its pharmacological effect through the enhancement of PAF-AH I and PPARγ expression in

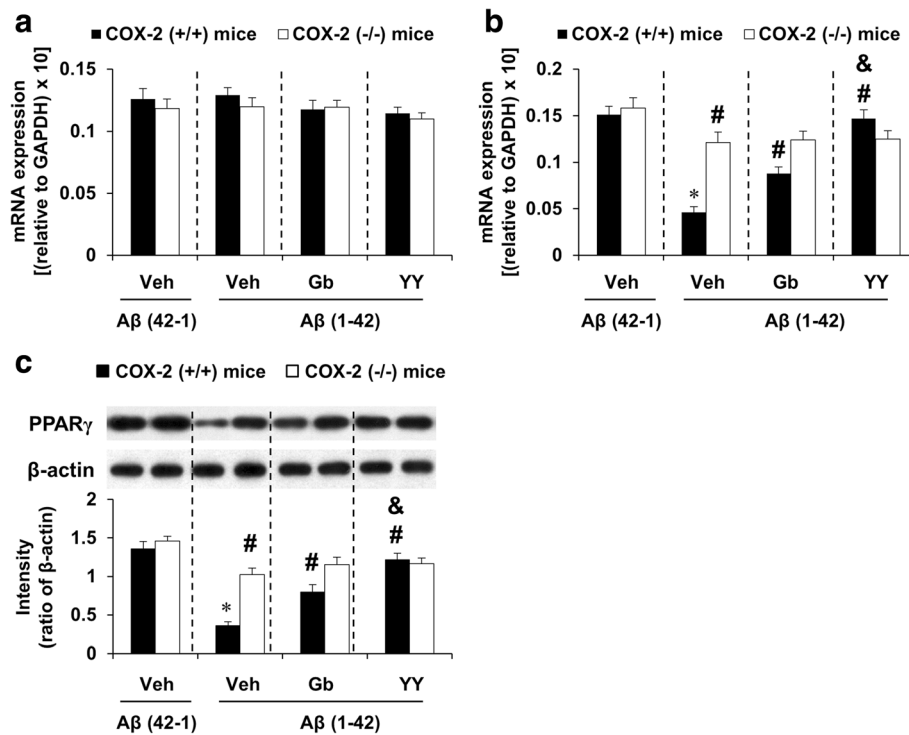


Fig. 8 Effects of YY-1224 (YY) or Gb on Aβ (1-42)-induced PPAR expressions in the hippocampi of mice. **a** Changes in PPARα mRNA expression. **b** Changes in PPARγ mRNA expression. **c** Changes in PPARγ protein expression. Veh vehicle for YY or Gb (10% tween-80 in sterile saline). Each value is the mean ± S.E.M of six animals. * $P < 0.01$ vs. COX-2 (+/+) mice treated with vehicle + Aβ (42-1); # $P < 0.01$ vs. COX-2 (+/+) mice treated with vehicle + Aβ (1-42); & $P < 0.05$ vs. COX-2 (+/+) mice treated with Gb + Aβ (1-42) (three-way ANOVA was followed by Fisher's LSD pairwise comparisons)

Aβ (1-42)-treated mice, we examined the effect of YY-1224 on the mRNA and protein expression of PAF-AH I and PPARγ in the hippocampus of APP/PS1 Tg mice. In line with the results from Aβ-treated mice, ANOVA and post hoc pairwise comparisons indicated that PAF-AH I-immunoreactivity was significantly increased by YY-1224 (Fig. 10a, b, $P < 0.05$ for CA1 and CA3), Gb (Fig. 10a, $P < 0.05$ for CA1), and pharmacological inhibition (i.e., meloxicam) of COX-2 (Fig. 10a, b, $P < 0.05$ for CA1 and CA3) in APP/PS1 Tg mice. Since the α2 subunit of PAF-AH I was positively regulated by YY-1224 in Aβ-treated mice, we examined the mRNA expression of this subunit in APP/PS1 Tg mice. ANOVA and post hoc pairwise comparisons revealed that the mRNA expression of the PAF-AH I α2 subunit was significantly enhanced by YY-1224 (Fig. 10c, $P < 0.01$), Gb (Fig. 10c, $P < 0.01$), and COX-2 inhibition (i.e., meloxicam; Fig. 10c, $P < 0.01$). YY-1224 enhanced PAF-AH I-immunoreactivity and PAF-AH I α2 mRNA expression more than Gb (Fig. 10a–c, ANOVA and post hoc pairwise comparisons showing the difference between Gb and YY-1224, $P < 0.05$). The results from RT-rt-PCR of PAF-AH I α2 subunit mRNA expression were comparable to those from RT-PCR (Additional file 1: Figure S11a).

As shown in Fig. 11, ANOVA and post hoc pairwise comparisons showed that the mRNA and protein expressions of PPARγ were significantly increased by treatment with YY-1224 (Fig. 11b, c, $P < 0.01$), Gb (Fig. 11b, c, $P < 0.01$ for mRNA, $P < 0.05$ for protein), or meloxicam (Fig. 11b, c, $P < 0.01$) in APP/PS1 Tg mice, and these results were consistent with the results from Aβ-treated mice. The pharmacological action of YY-1224 was more effective than that of Gb in PPARγ protein expression (Fig. 11c, ANOVA and post hoc pairwise comparisons showing the difference between Gb and YY-1224, $P < 0.05$). In addition, meloxicam did not affect the expression of PAF-AH or PPARγ in YY-1224- or Gb-treated APP/PS1 Tg mice (Figs. 10 and 11). The results from RT-rt-PCR of PPARα or PPARγ mRNA expression were comparable to those from RT-PCR (Additional file 1: Figure S11b and c).

Effects of meloxicam on the pharmacological activity of YY-1224 in response to reactive microgliosis in APP/PS1 Tg mice

To elucidate the role of microglia in the pharmacological effects of YY-1224, we examined the effect of Gb and YY-1224 on activated patterns of microglia (Fig. 12). Treatment with Gb and YY-1224 significantly attenuated

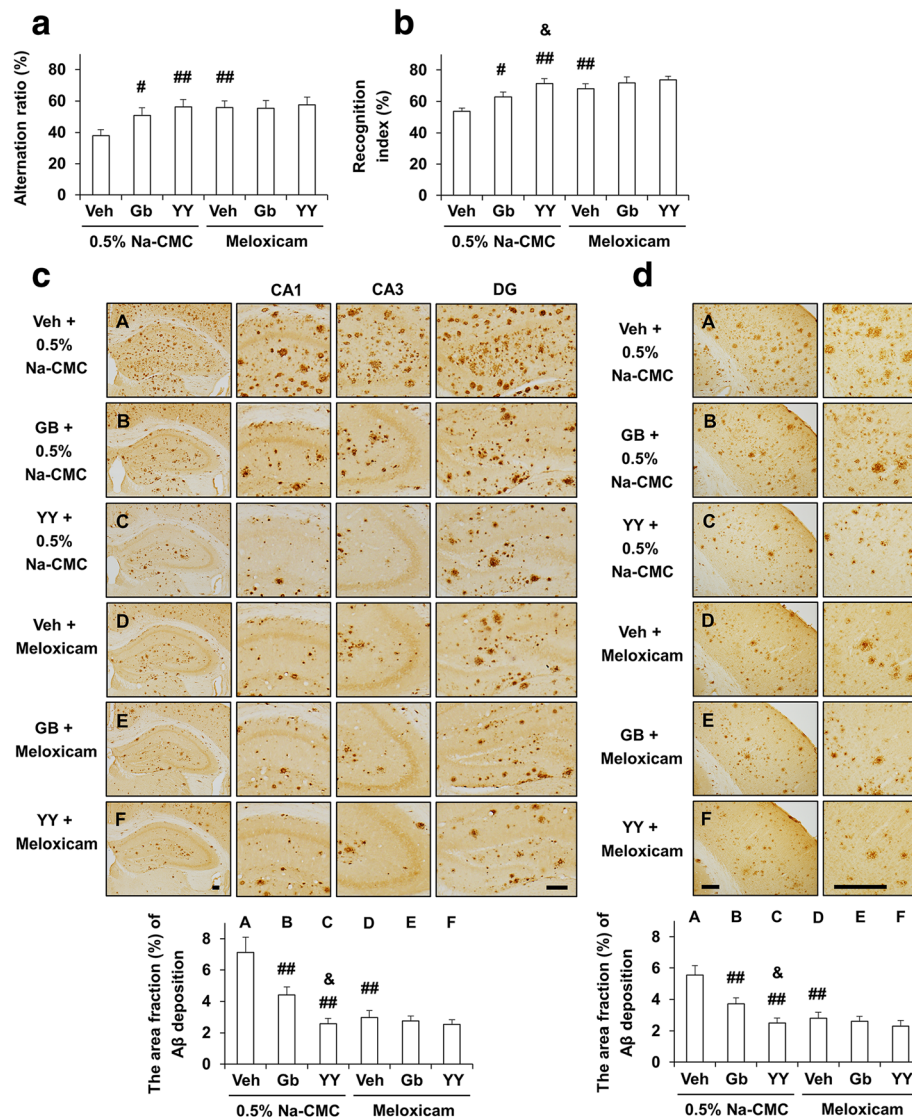


Fig. 9 Activity of YY-1224 (YY) or Gb on memory impairment and Aβ deposition in APP/PS1 Tg mice. **a** Effects of meloxicam on the pharmacological activity of YY or Gb in response to Y-maze performance and **b** novel object recognition. **c, d** Effect of meloxicam on the pharmacological activity of YY or Gb in response to Aβ-immunoreactivity in the hippocampus (**c**) and cortex (**d**). Veh vehicle for YY or Gb (10% tween-80 in sterile saline). Each value is the mean ± S.E.M of 10 (**a, b**) or 5 (**c, d**) animals. [#]*P* < 0.05, ^{##}*P* < 0.01 vs. vehicle + 0.5% Na-CMC; & *P* < 0.05 vs. Gb + 0.5% Na-CMC (two-way ANOVA was followed by Fisher's LSD pairwise comparisons). Scale bar = 200 μm

Iba-1-labeled microglia in the hippocampus and cerebral cortex of 0.5% Na-CMC-treated APP/PS1 Tg mice (Fig. 12a, b, ANOVA and post hoc pairwise comparisons showing the inhibitory effect of YY-1224, Gb, and meloxicam, *P* < 0.01 for hippocampus and cortex). Meloxicam did not alter significantly the Iba-1 immunoreactivity mediated by YY-1224 or Gb in APP/PS1 Tg mice (Fig. 12).

Different roles of microglia in tissue repair or damage may be due to distinct microglial subsets, i.e., “classically activated” pro-inflammatory (M1) or “alternatively activated” anti-inflammatory (M2) cells. Treatment with Gb or YY-1224 significantly decreased mRNA levels of M1

markers (CD16, CD32, and CD86) in the hippocampus of 0.5% Na-CMC-treated APP/PS1 Tg mice (Fig. 13a–c, ANOVA and post hoc pairwise comparisons showing the inhibitory effect of YY-1224 and Gb, *P* < 0.01). In contrast, Gb and YY-1224 significantly enhanced the mRNA levels of YM1 and CD206 of the M2 phenotype in the hippocampus of 0.5% Na-CMC-treated APP/PS1 Tg mice (Fig. 13d, e, ANOVA and post hoc pairwise comparisons showing the inhibitory effect of YY-1224 and Gb, *P* < 0.01). In meloxicam-treated groups, mRNA levels of CD16, CD32, and CD86 were significantly decreased in the hippocampus, while YM1 and CD206

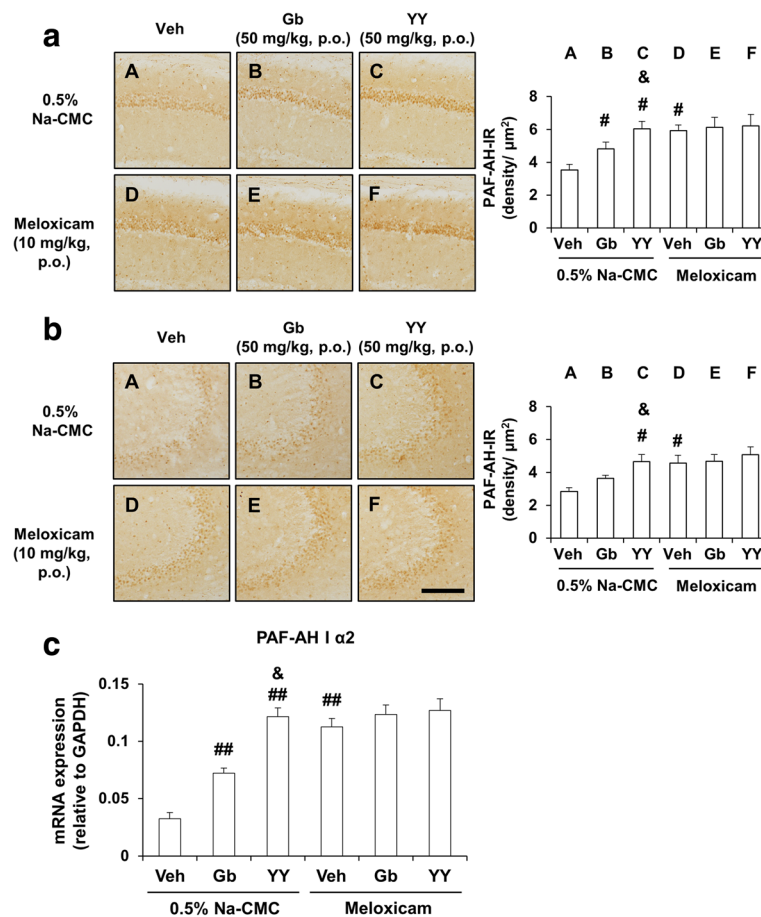


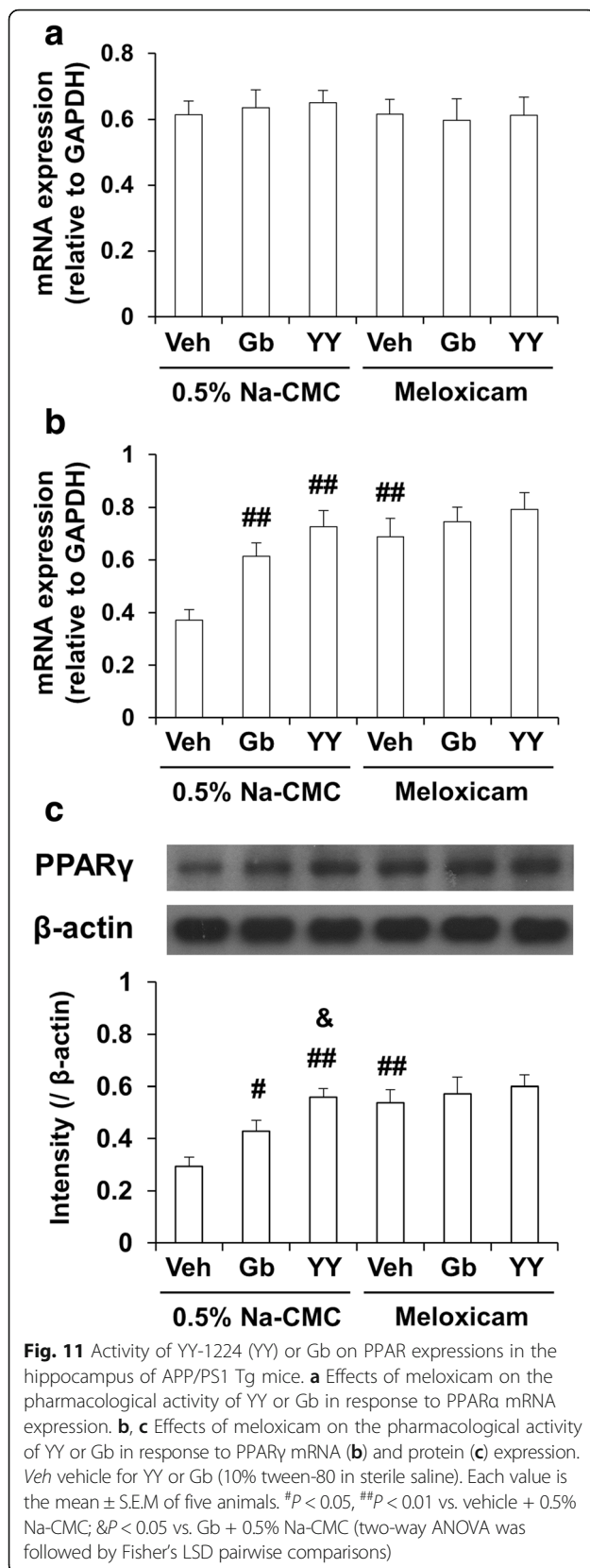
Fig. 10 Activity of YY-1224 (YY) or Gb on PAF-AH level in the hippocampus of APP/PS1 Tg mice. **a, b** Effects of meloxicam on the pharmacological activity of YY or Gb in response to PAF-AH-immunoreactivity in the CA1 (**a**) and CA3 (**b**) regions of the hippocampus. **c** Effects of meloxicam on the pharmacological activity of YY or Gb in response to PAF-AH I α2 mRNA expression in the hippocampus. Veh vehicle for YY or Gb (10% tween-80 in sterile saline). Each value is the mean \pm S.E.M of five animals. # $P < 0.05$, ## $P < 0.01$ vs. vehicle + 0.5% Na-CMC; & $P < 0.05$ vs. Gb + 0.5% Na-CMC (two-way ANOVA was followed by Fisher's LSD pairwise comparisons). Scale bar = 200 μ m

mRNA levels were significantly increased (Fig. 13, ANOVA and post hoc pairwise comparisons showing the inhibitory effect of meloxicam, $P < 0.01$). In addition, meloxicam did not significantly alter the mRNA expression of CD16, CD32, CD86, YM1, and CD206 mediated by YY-1224 or Gb in APP/PS1 Tg mice (Fig. 13). The results from RT-rt-PCR of the mRNA expression of microglial phenotypic markers were comparable to those from RT-PCR (Additional file 1: Figure S12).

Discussion

Increasing evidence has shown that A β -triggered microglial inflammatory activation damages neurons in AD pathogenesis [5, 57]. In this study, YY-1224 improved cognitive function and inhibited neuroinflammatory activation in COX-2 (+/+) mice after A β (1-42) treatment. YY-1224 inhibited the production of pro-inflammatory factors and oxidative stress through PAFR antagonism

and activation of the PPAR γ -COX-2 signaling pathway. YY-1224 appeared to be more effective than Gb against cognitive dysfunction and A β pathology in APP/PS1 Tg mice as well as against A β -induced memory impairment via microglia polarization. Previous studies have suggested that the antioxidant activity of Gb contributes to a memory-enhancing effect in AD patients or aged rats [58, 59]. Like NSAIDs, the constituents of Gb attenuated the production of inflammatory mediators such as COX-2, iNOS, and TNF- α in vitro [60]. We hypothesize that YY-1224 facilitates memory-enhancing and anti-inflammatory effects by increasing the ratio of terpenoids such as bilobalide and ginkgolides [36]. Bilobalide has been reported to exert protective effects on neurons [37–40], to facilitate synaptic transmission and plasticity in hippocampal subfields [61, 62], and to enhance spatial learning and memory [63]. Ginkgolide B exerts neuroprotection by alleviating neurotoxicity [42] and neuronal apoptosis [41], in addition to acting as a PAF antagonist [64].



PAF is a highly active phospholipid mediator of inflammation [65]. The initial step of PAF formation is activation of phospholipase A2 (PLA2) in a calcium-dependent manner, yielding lyso-PAF. During this step, arachidonic acid is also released and can be converted to its respective cyclooxygenase and lipoxygenase products. The lyso-PAF is then acetylated in position 2 of the glycerol backbone by a coenzyme A (CoA)-dependent acetyltransferase. The majority of PAF's effects are attributed to interaction with PAFR, which is expressed by multiple peripheral cell types; however, the effects of PAF are regionally restricted to microglia subpopulations in the CNS [66]. The inhibition of PAF activity is mediated by a deacetylation reaction catalyzed by PAF-AH [19]. PAF-AH I, originally identified in the brain, consists of three subunits ($\alpha 1$, $\alpha 2$, and β), in which the α subunits provide the catalytic activity. The complex has received attention in part because the subunit that modulates enzymatic activity (the β subunit) is the product of the LIS1 gene. LIS1 expression may be related to the regulation of PAF AH activity in the brain [67]. PAF-AH I has been implicated in neuronal development, neuronal functions, Alzheimer's disease, bipolar disorder, and tolerance to hypoxia [68]. Although the most structurally well-characterized component of PAF AH I is the $\alpha 1$ subunit [69], a highly specific role of the $\alpha 2$ subunit for PAF hydrolysis has been recognized [70]. In this study, the $\alpha 2$ subunit was the most sensitive to A β (1-42) exposure or double transgenic overexpression of APP and PS1. Therefore, the $\alpha 2$ subunit may be a therapeutic target for YY-1224 or Gb in response to A β (1-42) exposure or double transgenic overexpression of APP and PS1 via positive modulation of COX-2.

Among two major groups of constituents of YY-1224, flavonoid (24%) and terpenoid (12%) ginkgolides are known as potent antagonists of PAF [33]. YY-1224 treatment significantly attenuated decreases in the mRNA expression of PAF-AH I $\alpha 2$ and PAFR in response to A β (1-42) in COX-2 (+/+) mice. This suggests that the induction of PAF-AH I $\alpha 2$ and the PAF antagonistic activity of YY-1224 may contribute to its protective effects against A β (1-42) toxicity and possibly the double transgenic overexpression of APP and PS1.

Our current findings are consistent with previous reports that activation of PPAR γ regulates the expression of PAF-AH [71]. We also observed that repeated treatment with YY-1224 attenuates the A β (1-42)-induced decrease in PPAR γ and PAF-AH expression in COX-2 (+/+) but not COX-2 (-/-) mice, suggesting that the PPAR γ -PAF-AH pathway may mediate the protective effects of YY-1224 via positive modulation of COX-2. This notion is supported by previous findings that PAF induces the expression of COX-2 [72]. The connection between PAF and PGE2 production by COX-2 has also been demonstrated in astrocytes. Stimulation of these

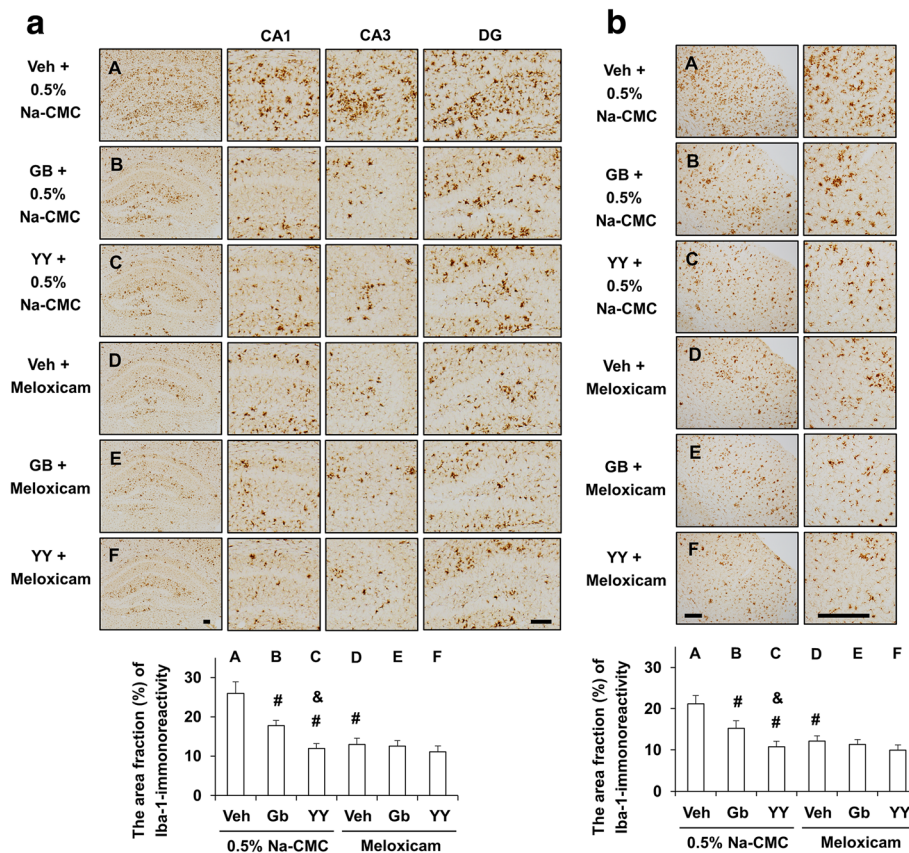


Fig. 12 Activity of YY-1224 (YY) or Gb on Iba-1-immunoreactivity in the APP/PS1 Tg mice. **a, b** Effects of meloxicam on the pharmacological activity of YY or Gb in response to Iba-1-immunoreactivity in the hippocampus (**a**) and cortex (**b**). Veh vehicle for YY or Gb (10% tween-80 in sterile saline). Each value is the mean \pm S.E.M of five animals. # $P < 0.01$ vs. vehicle + 0.5% Na-CMC; & $P < 0.05$ vs. Gb + 0.5% Na-CMC (two-way ANOVA was followed by Fisher's LSD pairwise comparisons). Scale bar = 200 μ m

cells with the non-hydrolyzable analog methylcarbamylo-PAF increased the secretion of PGE₂, which was reduced by inhibitors of COX-2 but not COX-1 [73]. In this manner, PAF, which is a short-lived molecule due to its rapid degradation by PAF-AH, is able to have a long lasting effect on neurons through induction of COX-2. We found that the deleterious effect of A β (1-42) on brain oxidative stress and inflammatory markers are found in COX-2 expressing- but not COX-2-null mice. In addition, the protective effect of YY-1224 is present only in COX-2 expressing- but not COX-2 null mice or APP/PS1 Tg mice treated with the selective COX-2 inhibitor, meloxicam. This suggests an important role of the PPAR-PAF-COX-2 pathway in the deleterious effect of A β (1-42) as well as beneficial effects of ginkgolides and YY-1224. Inhibition of this pathway could reduce the formation of pro-inflammatory products of COX-2 such as prostaglandins resulting in decreased levels of pro-inflammatory mediators. We also found that COX-2 inhibition might interfere with a possible feedforward loop to amplify the inflammatory process by reducing PAF signaling through induction of its degrading enzyme, PAF-AH I, and reduction in expression of the PAF

receptor, PAFR. This potential feedforward loop could exist in parallel with a previously described feedback loop, where pro-inflammatory mediators formed by COX-2 induce the expression of PAF-AH, resulting in reduced PAF and resolution of inflammation [74]. In this context, it is interesting to note that unlike PAF-AH I, PAF-AH II is induced by A β (1-42), and such induction is abolished in COX-2 null mice, although this enzyme is highly expressed in the liver and kidney [75]. More studies are needed to determine how COX-2 metabolites such as prostaglandins differentially regulate PAF-AH isoforms, resulting in propagation or modulation of inflammation.

Besides its effects on neurons, A β can activate microglial cells. This could lead to neuroinflammation and progression of neurodegeneration [76]. Microglia/macrophages are capable of undergoing phenotypic polarization to the M1 phenotype to produce pro-inflammatory cytokines, or to the M2 phenotype to produce anti-inflammatory cytokines [77, 78]. A prevalence of M1 over M2 microglia/macrophages has been reported in neurodegenerative pathologies, such as AD, and in the elderly brain [79]. In the present study, A β (1-42) induced an increase in

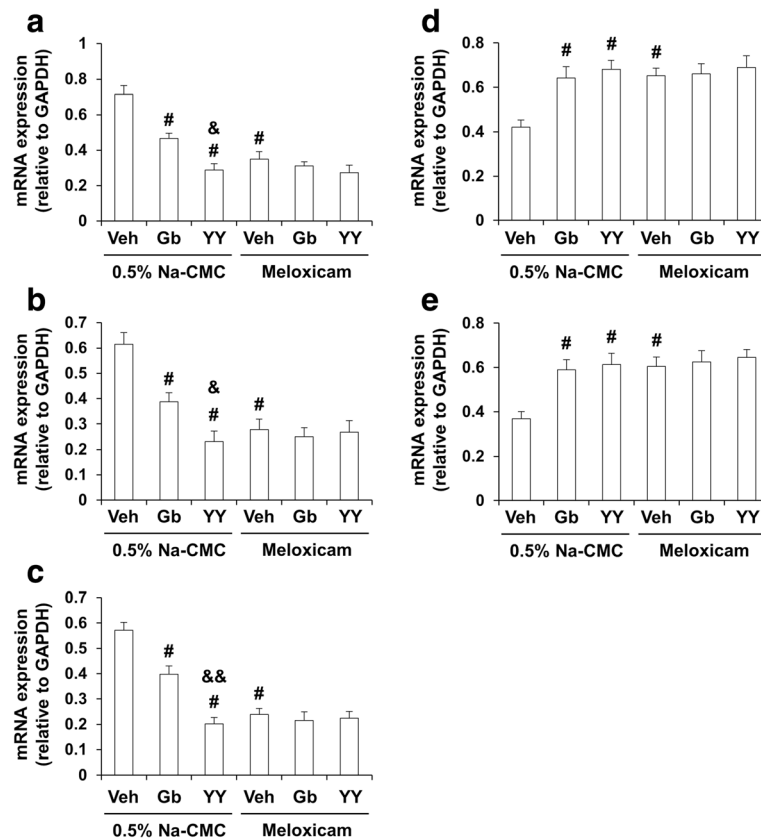


Fig. 13 Activity of YY-1224 (YY) or Gb on mRNA expressions of microglial phenotype in the hippocampus. **a–c** Effect of meloxicam on the pharmacological activity of YY or Gb in response to CD16 (**a**), CD32 (**b**), and CD86 (**c**) mRNA expressions of M1 phenotype microglia/macrophages. **d, e** Effect of meloxicam on the pharmacological activity of YY or Gb in response to YM1 (**d**) and CD206 (**e**) mRNA expressions of M2 phenotype microglia/macrophages. Veh vehicle for YY or Gb (10% tween-80 in sterile saline). Each value is the mean \pm S.E.M of five animals. # $P < 0.01$ vs. vehicle + 0.5% Na-CMC; & $P < 0.05$, && $P < 0.01$ vs. Gb + 0.5% Na-CMC (two-way ANOVA was followed by Fisher's LSD pairwise comparisons)

inflammatory cytokines including TNF- α and IL-1 β in microglia from the COX-2 (+/+) mice. PPAR γ agonists are able to prevent the detrimental polarization of microglia, or switch the polarization of reactive microglia from the pro-inflammatory to the anti-inflammatory phenotype [87, 80]. Therefore, our results suggest that inhibiting the M1 pro-inflammatory phenotype or activating microglial polarization toward an M2 anti-inflammatory phenotype might contribute to the memory-enhancing effect of YY-1224.

The results of this study are consistent with the notion that YY-1224 is a potential PPAR γ agonist that could be useful in the treatment of AD. PPAR γ agonists have potent anti-inflammatory activity [81, 82], and activation prevents brain damage through an anti-inflammatory effect on endothelial cells, astrocytes, and microglia [83]. Activation of nuclear factor kappa-light-chain-enhancer of activated B cells (NF- κ B) and COX-2 increases expression of pro-inflammatory cytokines [84–87], whereas inhibition of NF- κ B suppresses the expression of COX-2 induced by A β (25–35) in PC12 cells [87]. In contrast to

NF- κ B, activation of PPAR γ inhibits the expression of pro-inflammatory cytokines such as TNF- α , IL-1 β , and IL-6 in vitro [88, 89]. Treatment with a PPAR γ agonist 15dPGJ2 inhibited NF- κ B signaling and the DNA-binding activity of NF- κ B in macrophages [90, 91]. Moreover, treatment with another PPAR γ agonist, pioglitazone, attenuates the production of A β plaque burden and glial inflammation in the APPV717I transgenic mice [83] and cognitive impairments in AD patients [92].

Conclusions

In conclusion, we have demonstrated that terpene trilactone-activating *G. biloba* YY-1224 ameliorates AD pathogenesis by inhibiting oxidative stress and neuroinflammation via positive modulation of microglial activation. These protective effects of YY-1224 were mediated by its PAF antagonistic potential and PPAR γ activity through the COX-2 regulatory signaling pathway. Thus, YY-1224 may be a potential candidate for development of novel drugs for AD-like neurodegenerative disorders.

Additional files

Additional file 1: Supplemental figures. **Figure S1.** Representative HPLC chromatograms of ginkgo flavone glycosides and terpene trilactones. **Figure S2.** Experimental design for evaluating the effects of YY-1224 on A β (1-42)-induced learning impairments in COX-2 (+/+) and COX-2 (-/-) mice. **Figure S3.** Effects of YY-1224 or Gb on changes in the protein expression of BDNF, GDNF, NGF, or IGF-1 after k252a or JB-1 treatment in the hippocampus of the COX-2 (+/+) mice. **Figure S4.** Effects of YY-1224 or Gb on changes in SOD-1 or GPx-1 protein expression after DDC or MS treatment in the hippocampi of the COX-2 (+/+) mice. **Figure S5.** Effect of YY-1224 or Gb on changes in COX-2 mRNA expression in the hippocampi of the COX-2 (+/+) mice and on changes in COX-2 protein expression in PC12 cells or mixed cortical cells after treatment with A β (1-42). **Figure S6.** Effect of YY-1224 or Gb on A β (1-42)-induced cell death in PC12 cells or mixed cortical cells. **Figure S7.** Effects of YY-1224 or Gb on A β (1-42)-induced memory impairment in COX-2 (+/+) and COX-2 (-/-) mice. **Figure S8.** Effects of YY-1224 or Gb on A β (1-42)-induced changes in PAFR and PAF-AH mRNA levels in the hippocampus. **Figure S9.** Effects of YY-1224 or Gb on A β (1-42)-induced pro-inflammatory genes in the hippocampi of mice. **Figure S10.** Effects of YY-1224 or Gb on A β (1-42)-induced PPAR mRNA expressions in the hippocampi of mice. **Figure S11.** Effects of YY-1224 or Gb on the mRNA level of PAF-AH I α 2 and PPAR in the hippocampus of APP/PS1 Tg mice. **Figure S12.** Effects of YY-1224 or Gb on mRNA expressions of microglial phenotype markers in the hippocampus. **Figure S13.** Schematic illustration of the image analysis to quantify the area of A β deposition or Iba-1-immunoreactivity. Detailed figure legends are included in the additional file 2. (PDF 5615 kb)

Additional file 2: Supplemental information. (DOCX 74 kb)

Abbreviations

4-HNE: 4-Hydroxy-2-nonenal; AD: Alzheimer's disease; ANOVA: Analysis of variance; APP/PS1 Tg: APP^{swe}/PS1^{dE9} transgenic; A β : β -amyloid; CNS: Central nervous system; CoA: Coenzyme A; COX: Cyclooxygenase; Gb: *G. biloba* extract; IFN- γ : Interferon gamma; IL-1 β : Interleukin-1 beta; IL-6: Interleukin-6; iNOS: Inducible NO synthase; lysoPAF: 1-O-alkyl-sn-glycero-3-phosphocholine; MDA: Malondialdehyde; Na-CMC: Sodium carboxymethyl cellulose; NF- κ B: Nuclear factor kappa-light-chain-enhancer of activated B cells; NO: Nitric oxide; NSAIDs: Nonsteroidal anti-inflammatory drugs; PAF: Platelet-activating factor; PAF-AH: PAF acetylhydrolase; PGE2: Prostaglandin E2; PLA2: Phospholipase A2; PPAR: Peroxisome proliferator-activated receptor; ROS: Reactive oxygen species; RT-PCR: Reverse transcription and polymerase chain reaction; TNF- α : Tumor necrosis factor alpha

Acknowledgements

The English in this document has been checked by at least two professional editors, both native speakers of English (eWorldEditing, Inc., Eugene, OR 97401, USA).

Funding

This study is supported by a grant (No.S111415L020100) of the "Forestry Technology Projects" (provided by the Korea Forest Service), and in part supported by Basic Science Research Program through the National Research Foundation of Korea (NRF) funded by the Ministry of Science, ICT & Future Planning (#NRF-2013R1A1A2060894 and #NRF-2016R1A1A1A05005201), Republic of Korea. DK Dang was supported by the BK21 PLUS program, NRF, Republic of Korea.

Availability of data and materials

Not applicable.

Authors' contributions

ZYL, YHC, EJS, DKD, and JHJ took part in the pilot studies with the animal treatment. SKK, SYN, and TGB worked for the purification and stability of YY-1224. JHJ, WYO, and TN provided critical comments for the discussion and revision. ZYL, YHC, and DKD performed the main experiment and histology. EJS and HCK arranged this manuscript via full communications with all co-authors. All authors read and approved the final version of this manuscript.

Competing interests

The authors declare that they have no competing interests.

Consent for publication

Not applicable.

Ethics approval and consent to participate

All animals were treated in accordance with the Guide for the care and use of laboratory animals (National Research Council of the National Academies, 2011). The present study was performed in accordance with the Institute for Laboratory Research (ILAR) Guidelines for the Care and Use of Laboratory Animals.

Publisher's Note

Springer Nature remains neutral with regard to jurisdictional claims in published maps and institutional affiliations.

Author details

¹Neuropsychopharmacology and Toxicology Program, College of Pharmacy, Kangwon National University, Chunchon 24341, Republic of Korea. ²Department of Anatomy, College of Medicine, Chung-Ang University, Seoul 06974, Republic of Korea. ³Department of Pharmacology, College of Medicine, Chung-Ang University, Seoul 06974, Republic of Korea. ⁴Department of Oriental Medical Food and Nutrition, Semyung University, Jecheon 27136, Republic of Korea. ⁵Ginsentology Research Laboratory and Department of Physiology, College of Veterinary Medicine and Bio/Molecular Informatics Center, Konkuk University, Seoul 05029, Republic of Korea. ⁶R&D Center, Yuyu Pharma, Seoul 04598, Republic of Korea. ⁷Department of Psychiatry, Medical School, Kangwon National University, Chunchon 24341, Republic of Korea. ⁸Department of Anatomy, National University of Singapore, Singapore 119260, Singapore. ⁹Nabeshima Laboratory, Graduate School of Pharmaceutical Sciences, Meijo University, Nagoya 468-8503, Japan.

Received: 8 November 2016 Accepted: 18 April 2017

Published online: 27 April 2017

References

- Mouri A, Noda Y, Hara H, Mizoguchi H, Tabira T, Nabeshima T. Oral vaccination with a viral vector containing Abeta cDNA attenuates age-related Abeta accumulation and memory deficits without causing inflammation in a mouse Alzheimer model. *FASEB J*. 2007;21:2135-48.
- Tsunekawa H, Noda Y, Mouri A, Yoneda F, Nabeshima T. Synergistic effects of selegiline and donepezil on cognitive impairment induced by amyloid beta (25-35). *Behav Brain Res*. 2008;190:224-32.
- Lu P, Mamiya T, Lu LL, Mouri A, Zou L, Nagai T, Hiramatsu M, Ikejima T, Nabeshima T. Silibinin prevents amyloid beta peptide-induced memory impairment and oxidative stress in mice. *Br J Pharmacol*. 2009;157:1270-77.
- Yamada K, Nabeshima T. Animal models of Alzheimer's disease and evaluation of anti-dementia drugs. *Pharmacol Ther*. 2000;88:93-113.
- Akiyama H, Barger S, Barnum S, Bradt B, Bauer J, Cole GM, Cooper NR, Eikelenboom P, Emmerling M, Fiebich BL, Finch CE, Frautschy S, Griffin WS, Hampel H, Hull M, Landreth G, Lue L, Mrak R, Mackenzie IR, McGeer PL, O'Banion MK, Pachter J, Pasinetti G, Plata-Salaman C, Rogers J, Rydel R, Shen Y, Streit W, Strommeyer R, Tooyoma I, Van Muiswinkel FL, Veerhuis R, Walker D, Webster S, Wegryniak B, Wenk G, Wyss-Coray T. Inflammation and Alzheimer's disease. *Neurobiol Aging*. 2000;21:383-421.
- Rogers J, Kirby LC, Hempelman SR, Berry DL, McGeer PL, Kaszniak AW, Zalsinski J, Cofield M, Mansukhani L, Willson P. Clinical trial of indomethacin in Alzheimer' disease. *Neurology*. 1993;43:1609-11.
- Rich JB, Rasmussen DX, Folstein MF, Carson KA, Kawas C, Brandt J. Nonsteroidal anti-inflammatory drugs in Alzheimer's disease. *Neurology*. 1995;45:51-5.
- Pasinetti GM, Aisen PS. Cyclooxygenase-2 expression is increased in frontal cortex of Alzheimer's disease brain. *Neuroscience*. 1998;87:319-24.
- Pasinetti GM. From epidemiology to therapeutic trials with anti-inflammatory drugs in Alzheimer's disease: the role of NSAIDs and cyclooxygenase in beta-amyloidosis and clinical dementia. *J Alzheimer Dis*. 2002;4:435-45.
- Ishii S, Schimizu T. Platelet activating factor (PAF) receptor and genetically engineered PAF receptor mutant mice. *Prog Lipid Res*. 2000;39:41-82.

11. Bazan NG, Fletcher BS, Herschman HR, Mukherjee PK. Platelet-activating factor and retinoic acid synergistically activate the inducible prostaglandin synthase gene. *Proc Natl Acad Sci U S A*. 1994;91:5252–56.
12. MacLennan KM, Smith PF, Darlington CL. Platelet-activating factor in the CNS. *Prog Neurobiol*. 1996;50:585–96.
13. Bennett S, Chen J, Pappas BA, Roberts DC, Tenniswood M. Platelet activating factor receptor expression is associated with neuronal apoptosis in an in vivo model of excitotoxicity. *Cell Death Differ*. 1998;5:867–75.
14. Kim BK, Shin EJ, Kim HC, Chung YH, Dang DK, Jung BD, Park DH, Wie MB, Kim WK, Shimizu T, Nabeshima T, Jeong JH. Platelet-activating factor receptor knockout mice are protected from MPTP-induced dopaminergic degeneration. *Neurochem Int*. 2013;63:121–32.
15. Bito H, Honda Z, Nakamura M, Shimizu T. Cloning, expression and tissue distribution of rat platelet-activating factor receptor cDNA. *Eur J Biochem*. 1994;221:211–8.
16. Pei Y, Barber LA, Murphy RC, Johnson CA, Kelly SW, Dy LC, Fertel RH, Nguyen TM, Williams DA. Activation of the epidermal platelet-activating factor receptor results in cytokine and cyclooxygenase-2 biosynthesis. *J Immunol*. 1998;161:1954–61.
17. Teather LA, Packard MG, Bazan NG. Differential interaction of platelet-activating factor and NMDA receptor function in hippocampal and dorsal striatal memory processes. *Neurobiol Learn Mem*. 2001;75:310–24.
18. Teather LA, Magnusson JE, Chow CM, Wurtman RJ. Environmental conditions influence hippocampus-dependent behaviours and brain levels of amyloid precursor protein in rats. *Eur J Neurosci*. 2002;16:2405–15.
19. Arai H. Platelet-activating factor acetylhydrolase. *Prostaglandins Other Lipid Mediat*. 2002;68:69:83–94.
20. Blank ML, Lee T, Fitzgerald V, Snyder F. A specific acetylhydrolase for 1-alkyl-2-acetyl-sn-glycero-3-phosphocholin (a hypotensive and platelet-activating lipid). *J Biol Chem*. 1981;256:175–8.
21. Karasawa K, Harada A, Satoh N, Inoue K, Setaka M. Plasma platelet activating factor-actylhydrolase (PAF-AH). *Prog Lipid Res*. 2003;42:93–114.
22. Heneka MT, Klockgether T, Feinstein DL. Peroxisome proliferator-activated receptor-gamma ligands reduce neuronal inducible nitric oxide synthase expression and cell death in vivo. *J Neurosci*. 2000;20:6862–7.
23. de la Monte SM, Wands JR. Molecular indices of oxidative stress and mitochondrial dysfunction occur early and often progress with severity of Alzheimer's disease. *J Alzheimers Dis*. 2006;9:167–81.
24. Combs CK, Johnson DE, Karlo JC, Cannady SB, Landreth GE. Inflammatory mechanisms in Alzheimer's disease: inhibition of beta-amyloid-stimulated proinflammatory responses and neurotoxicity by PPARgamma agonists. *J Neurosci*. 2000;20:558–67.
25. Yan Q, Zhang J, Liu H, Babu-Khan S, Vassar R, Biere AL, Citron M, Landreth G. Anti-inflammatory drug therapy alters beta-amyloid processing and deposition in an animal model of Alzheimer's disease. *J Neurosci*. 2003;23:7504–9.
26. Kwon YS, Ann HS, Nabeshima T, Shin EJ, Kim WK, Jhoo JH, Jhoo WK, Wie MB, Kim YS, Jang KJ, Kim HC. Selegiline potentiates the effects of EGb 761 in response to ischemic brain injury. *Neurochem Int*. 2004;45:157–70.
27. Zhang Z, Peng D, Zhu H, Wang X. Experimental evidence of Ginkgo biloba extract EGB as a neuroprotective agent in ischemia stroke rats. *Brain Res Bull*. 2012;87:193–8.
28. Wheatley D. Ginkgo biloba in the treatment of sexual dysfunction due to antidepressant drugs. *Hum Psychopharmacol Clin Exp*. 1999;14:512–3.
29. Luo Y. Ginkgo biloba neuroprotection: therapeutic implications in Alzheimer's disease. *J Alzheimers Dis*. 2001;3:401–7.
30. Ahlemeyer B, Krieglstein J. Neuroprotective effects of Ginkgo biloba extract. *Cell Mol Life Sci*. 2003;60:1779–92.
31. Herrschaft H, Nacu A, Likhachev S, Sholomov I, Hoerr R, Schlaefke S. Ginkgo biloba extract Egb 761(R) in dementia with neuropsychiatric features: a randomised, placebo-controlled trial to confirm the efficacy and safety of a daily dose of 240 mg. *J Psychiatr Res*. 2012;46:716–23.
32. Jin CH, Shin EJ, Park JB, Jang CG, Li Z, Kim MS, Koo KH, Yoon HJ, Park SJ, Choi WC, Yamada K, Nabeshima T, Kim HC. Fustin flavonoid attenuates beta-amyloid (1–42)-induced learning impairment. *J Neurosci Res*. 2009;87:3658–70.
33. Shi C, Zhao L, Zhu B, Li Q, Yew DT, Yao Z, Xu J. Protective effects of Ginkgo biloba extract (EGb761) and its constituents quercetin and ginkgolide B against beta-amyloid peptide-induced toxicity in SH-SY5Y cells. *Chem Biol Interact*. 2009;181:115–23.
34. Bourgain RH, Andries R, Esanu A, Braquet P. PAF-acether induced arterial thrombosis and the effect of specific antagonists. *Adv Exp Med Biol*. 1992; 316:427–40.
35. Kudolo GB, Dorsey S, Blodgett J. Effect of the ingestion of Ginkgo biloba extract on platelet aggregation and urinary prostanoid excretion in healthy and Type 2 diabetic subjects. *Thromb Res*. 2002;108:151–60.
36. Nam Y, Shin EJ, Shin SW, Lim YK, Jung JH, Lee JH, Ha JR, Chae JS, Ko SK, Jeong JH, Jang CG, Kim HC. YY162 prevents ADHD-like behavioral side effects and cytotoxicity induced by Aroclor1254 via interactive signaling between antioxidant potential, BDNF/TrkB, DAT and NET. *Food Chem Toxicol*. 2014;65:280–92.
37. Bruno C, Cuppini R, Sartini S, Cecchini T, Ambrogini P, Bombardelli E. Regeneration of motor nerves in bilobalide-treated rats. *Planta Med*. 1993;59:302–7.
38. Defeudis FV. Bilobalide and neuroprotection. *Pharmacol Res*. 2002;46:565–8.
39. Rossi R, Basilico F, Rossoni G, Riva A, Morazzoni P, Mauri PL. Liquid chromatography/atmospheric pressure chemical ionization ion trap mass spectrometry of bilobalide in plasma and brain of rats after oral administration of its phospholipidic complex. *J Pharm Biomed Anal*. 2009;50:224–7.
40. Tchantchou F, Lacor PN, Cao Z, Lao L, Hou Y, Cui C, Klein WL, Luo Y. Stimulation of neurogenesis and synaptogenesis by bilobalide and quercetin via common final pathway in hippocampal neurons. *J Alzheimers Dis*. 2009;18:787–98.
41. Xiao Q, Wang C, Li J, Hou Q, Ma J, Wang W, Wang Z. Ginkgolide B protects hippocampal neurons from apoptosis induced by beta-amyloid 25–35 partly via up-regulation of brain-derived neurotrophic factor. *Eur J Pharmacol*. 2010;647:48–54.
42. Zhang C, Tian X, Luo Y, Meng X. Ginkgolide B attenuates ethanol-induced neurotoxicity through regulating NADPH oxidases. *Toxicology*. 2011;287:124–30.
43. Feng ZH, Wang TG, Li DD, Fung P, Wilson BC, Liu B, Ali SF, Langenbach R, Hong JS. Cyclooxygenase-2-deficient mice are resistant to 1-methyl-4-phenyl-1, 2, 3, 6-tetrahydropyridine-induced damage of dopaminergic neurons in the substantia nigra. *Neurosci Lett*. 2002;329:354–8.
44. Morham SG, Langenbach R, Loftin CD, Tian HF, Vouloumanos N, Jennette JC, Mahler JF, Kluckman KD, Ledford A, Lee CA. Prostaglandin synthase 2 gene disruption causes severe renal pathology in the mice. *Cell*. 1995;83: 473–82.
45. Laursen SE, Belknap JK. Intracerebroventricular injections in mice. Some methodological refinements. *J Pharmacol Methods*. 1986;16:355–7.
46. Hwang SH, Shin EJ, Shin TJ, Lee BH, Choi SH, Kang J, Kim HJ, Kwon SH, Jang CG, Lee JH, Kim HC, Nah SY. Gintonin, a ginseng-derived lysophosphatidic acid receptor ligand, attenuates Alzheimer's disease-related neuropathies: involvement of non-amyloidogenic processing. *J Alzheimers Dis*. 2012;31:207–23.
47. Park SJ, Shin EJ, Min SS, An J, Li Z, Chung YH, Jeong JH, Bach JH, Nah SY, Kim WK, Jang CG, Kim YS, Nabeshima Y, Nabeshima T, Kim HC. Inactivation of JAK2/STAT3 signaling axis and downregulation of M1 mAChR cause cognitive impairment in klotho mutant mice, a genetic model of aging. *Neuropsychopharmacology*. 2013;38:1426–37.
48. Shin EJ, Chung YH, Le HL, Jeong JH, Dang DK, Nam Y, Wie MB, Nah SY, Nabeshima Y, Nabeshima T, Kim HC. Melatonin attenuates memory impairment induced by klotho gene deficiency via interactive signaling between MT2 receptor, ERK, and Nrf2-related antioxidant potential. *Int J Neuropsychopharmacol*. 2014. doi: 10.1093/ijnp/pyu105
49. Shin EJ, Jeong JH, Chung CK, Kim DJ, Wie MB, Park ES, Chung YH, Nam Y, Tran TV, Lee SY, Kim HJ, Ong WY, Kim HC. Ceruloplasmin is an endogenous protectant against kainate neurotoxicity. *Free Radic Biol Med*. 2015;84:355–72.
50. Dang DK, Shin EJ, Nam Y, Ryou S, Jeong JH, Jang CG, Nabeshima T, Hong JS, Kim HC. Apocynin prevents mitochondrial burdens, microglial activation, and pro-apoptosis induced by a toxic dose of methamphetamine in the striatum of mice via inhibition of p47phox activation by ERK. *J Neuroinflammation*. 2016;13:12.
51. Kim BK, Tran HY, Shin EJ, Lee C, Chung YH, Jeong JH, Bach JH, Kim WK, Park DH, Saito K, Nabeshima T, Kim HC. IL-6 attenuates trimethyltin-induced cognitive dysfunction via activation of JAK2/STAT3, M1 mAChR and ERK signaling network. *Cell Signal*. 2013;25:1348–60.
52. Richard MJ, Guiraud P, Meo J, Favier A. High-performance liquid chromatographic separation of malondialdehyde-thiobarbituric acid adduct in biological materials (plasma and human cells) using a commercially available reagent. *J Chromatogr*. 1992;577:9–18.
53. Tran HY, Shin EJ, Saito K, Nguyen XK, Chung YH, Jeong JH, Bach JH, Park DH, Yamada K, Nabeshima T, Yoneda Y, Kim HC. Protective potential of IL-6 against trimethyltin-induced neurotoxicity in vivo. *Free Radic Biol Med*. 2012;52:1159–74.

54. Oliver CN, Ahn BW, Moerman EJ, Goldstein S, Stadtman ER. Age-related changes in oxidized proteins. *J Biol Chem.* 1987;262:5488–91.
55. Whittaker VP, Michaelson IA, Kirkland RJ. The separation of synaptic vesicles from nerve-ending particles (synaptosomes). *Biochem J.* 1964;90:293–303.
56. Lebel CP, Bondy SC. Sensitive and rapid quantitation of oxygen reactive species formation in rat synaptosomes. *Neurochem Int.* 1990;17:435–40.
57. Wyss-Coray T, Rogers J. Inflammation in Alzheimer disease—a brief review of the basic science and clinical literature. *Cold Spring Harb Perspect Med.* 2012; doi: 10.1101/cshperspect.a006346
58. Wang Y, Wang L, Wu J, Cai J. The in vivo synaptic plasticity mechanism of EGb 761-induced enhancement of spatial learning and memory in aged rats. *Br J Pharmacol.* 2006;148:147–53.
59. Schulz V. Ginkgo extract or cholinesterase inhibitors in patients with dementia: what clinical trials and guidelines fail to consider. *Phytomedicine.* 2003;10:74–9.
60. Kotakadi VS, Jin Y, Hofseth AB, Ying L, Cui X, Volate S, Chumanovich A, Wood PA, Price RL, McNeal A, Singh UP, Singh NP, Nagarkatti M, Nagarkatti PS, Matesic LE, Auclair K, Wargovich MJ, Hofseth LJ. Ginkgo biloba extract EGb 761 has anti-inflammatory properties and ameliorates colitis in mice by driving effector T cell apoptosis. *Carcinogenesis.* 2008; 29:1799–806.
61. Suzuki E, Sato M, Takezawa R, Usuki T, Okada T. The facilitative effects of bilobalide, a unique constituent of Ginkgo biloba, on synaptic transmission and plasticity in hippocampal subfields. *J Physiol Sci.* 2011;61:421–7.
62. Huang M, Qian Y, Guan T, Huang L, Tang X, Li Y. Different neuroprotective responses of Ginkgolide B and bilobalide, the two Ginkgo components, in ischemic rats with hyperglycemia. *Eur J Pharmacol.* 2012;677:71–6.
63. Ma L, Wang S, Tai F, Yuan G, Wu R, Liu X, Wei B, Yang X. Effects of bilobalide on anxiety, spatial learning, memory and levels of hippocampal glucocorticoid receptors in male Kunming mice. *Phytomedicine.* 2012;20:89–96.
64. Hu L, Chen Z, Xie Y, Jiang Y, Zhen H. Alkyl and alkoxy-carbonyl derivatives of ginkgolide B: synthesis and biological evaluation of PAF inhibitory activity. *Bioorg Med Chem.* 2000;8:1515–21.
65. Prescott SM, McIntyre TM, Zimmerman GA. The role of platelet-activating factor in endothelial cells. *Thromb Haemost.* 1990;64:99–103.
66. Mori M, Aihara M, Kume K, Hamanoue M, Kohsaka S, Shimizu T. Predominant expression of platelet-activating factor receptor in rat brain microglia. *J Neurosci.* 2002;16:3590–600.
67. Shmueli O, Cahana A, Reiner O. Platelet-activating factor (PAF) acetylhydrolase activity, LIS1 expression, and seizures. *J Neurosci Res.* 1999;57:176–84.
68. Hattori M, Arai H. Intracellular PAF-acetylhydrolase type I. *Enzymes.* 2015;38:23–36.
69. Hattori M, Adachi H, Tsujimoto M, Arai H, Inoue K. The catalytic subunit of bovine brain platelet-activating factor acetylhydrolase is a novel type of serine esterase. *J Biol Chem.* 1994;269:23150–5.
70. Tjoelker LW, Stafforini DM. Platelet-activating factor acetylhydrolases in health and disease. *Biochim Biophys Acta.* 2000;1488:102–23.
71. Sumita C, Maeda M, Fujio Y, Kim J, Fujitsu J, Kasayama S, Yamamoto I, Azuma J. Pioglitazone induces plasma platelet activating factor-acetylhydrolase and inhibits platelet activating factor-mediated cytoskeletal reorganization in macrophage. *Biochim Biophys Acta.* 2004; 1673:115–21.
72. Bazan HE, Tao Y, DeCoster MA, Bazan NG. Platelet-activating factor induces cyclooxygenase-2 gene expression in corneal epithelium. Requirement of calcium in the signal transduction pathway. *Invest Ophthalmol Vis Sci.* 1997;38:2492–501.
73. Teather LA, Wurtman RJ. Cyclooxygenase-2 mediates platelet-activating factor-induced prostaglandin E2 release from rat primary astrocytes. *Neurosci Lett.* 2003;340:177–80.
74. Jung WK, Lee CM, Lee DS, Na G, Lee DY, Choi I, Park SG, Seo SK, Yang JW, Choi JS, Lee YM, Park WS, Choi IW. The 15-deoxy- δ 12,14-prostaglandin J2 inhibits LPS-stimulated inflammation via enhancement of the platelet-activating factor acetylhydrolase activity in human retinal pigment epithelial cells. *Int J Mol Med.* 2014;33:449–56.
75. Hattori K, Hattori M, Adachi H, Tsujimoto M, Arai H, Inoue K. Purification and characterization of platelet-activating factor acetylhydrolase II from bovine liver cytosol. *J Biol Chem.* 1995;270:22308–13.
76. Pisanu A, Lecca D, Mulas G, Wardas J, Simbula G, Spiga S, Carta AR. Dynamic changes in pro- and anti-inflammatory cytokines in microglia after PPAR- γ agonist neuroprotective treatment in the MPTP mouse model of progressive Parkinson's disease. *Neurobiol Dis.* 2014;71:280–91.
77. Varnum MM, Ikezu T. The classification of microglial activation phenotypes on neurodegeneration and regeneration in Alzheimer's disease brain. *Arch Immunol Ther Exp (Warsz).* 2012;60:251–66.
78. Shin EJ, Shin SW, Nguyen TT, Park DH, Wie MB, Jang CG, Nah SY, Yang BW, Ko SK, Nabeshima T, Kim HC. Ginsenoside Re rescues methamphetamine-induced oxidative damage, mitochondrial dysfunction, microglial activation, and dopaminergic degeneration by inhibiting the protein kinase C δ gene. *Mol Neurobiol.* 2014;49:1400–21.
79. Tang Y, Li T, Li J, Yang J, Liu H, Zhang XJ, Le W. Mjrd3 is essential for the epigenetic modulation of microglia phenotypes in the immune pathogenesis of Parkinson's disease. *Cell Death Differ.* 2014;21:369–80.
80. Mandrekar-Colucci S, Karlo JC, Landreth GE. Mechanisms underlying the rapid peroxisome proliferator-activated receptor- γ -mediated amyloid clearance and reversal of cognitive deficits in a murine model of Alzheimer's disease. *J Neurosci.* 2012;32:10117–28.
81. Gelman L, Fruchart JC, Auwerx J. An update on the mechanisms of action of the peroxisome proliferator-activated receptors (PPARs) and their roles in inflammation and cancer. *Cell Mol Life Sci.* 1999;55:932–43.
82. Ricote M, Huang JT, Welch JS, Glass CK. The peroxisome proliferator-activated receptor (PPAR γ) as a regulator of monocyte/macrophage function. *J Leukoc Biol.* 1999;66:733–9.
83. Heneka MT, Sastre M, Dumitrescu-Ozimek L, Hanke A, Dewachter I, Kuiperi C, O'Banion K, Klockgether T, Van Leuven F, Landreth GE. Acute treatment with the PPAR γ agonist pioglitazone and ibuprofen reduces glial inflammation and Abeta1-42 levels in APPV7171 transgenic mice. *Brain.* 2005;128:1442–53.
84. Quadros A, Patel N, Crescentini R, Crawford F, Paris D, Mullan M. Increased TNF α production and Cox-2 activity in organotypic brain slice cultures from APPsw transgenic mice. *Neurosci Lett.* 2003;353:66–8.
85. Chawla A, Barak Y, Nagy L, Liao D, Tontonoz P, Evans RM. PPAR- γ dependent and independent effects on macrophage-gene expression in lipid metabolism and inflammation. *Nat Med.* 2001;7:48–52.
86. Moore PE, Lahiri T, Laporte JD, Church T, Panettieri Jr RA, Shore SA. Selected contribution: synergism between TNF- α and IL-1 β in airway smooth muscle cells: implications for beta-adrenergic responsiveness. *J Appl Physiol.* 2001;91:1467–74.
87. Lukiw WJ, Bazan NG. Strong nuclear factor-kappaB-DNA binding parallels cyclooxygenase-2 gene transcription in aging and in sporadic Alzheimer's disease superior temporal lobe neocortex. *J Neurosci Res.* 1998;53:583–92.
88. Jiang C, Ting AT, Seed B. PPAR- γ agonists inhibit production of monocyte inflammatory cytokines. *Nature.* 1998;391:82–6.
89. Ricote M, Huang J, Fajas L, Li A, Welch J, Najib J, Witztum JL, Auwerx J, Palinski W, Glass CK. Expression of the peroxisome proliferator-activated receptor gamma (PPAR γ) in human atherosclerosis and regulation in macrophages by colony stimulating factors and oxidized low density lipoprotein. *Proc Natl Acad Sci U S A.* 1998;95:7614–9.
90. Rossi GP, Andreis PG, Neri G, Tortorella C, Pelizzo MR, Sacchetto A, Nussdorfer GG. Endothelin-1 stimulates aldosterone synthesis in Conn's adenomas via both A and B receptors coupled with the protein kinase C- and cyclooxygenase-dependent signaling pathways. *J Investing Med.* 2000;48:343–50.
91. Castrillo A, Diaz-Guerra MJ, Hortelano S, Martin-Sanz P, Bosca L. Inhibition of IkappaB kinase and IkappaB phosphorylation by 15-deoxy-Delta(12,14)prostaglandin J(2) in activated murine macrophages. *Mol Cell Biol.* 2000;20:1692–8.
92. Sato T, Hanyu H, Akai T, Takasaki A, Sakurai H, Iwamoto T. A patient with early Alzheimer's disease who showed improvement of cognitive function and cerebral perfusion by combined therapy of nilvadipine and PPAR gamma agonists. *Nippon Ronen Igakkai Zasshi.* 2008;45:428–33.
93. Overbergh L, Decallonne B, Branisteau DD, Valckx D, Kasran A, Bouillon R, Mathieu C. Acute shock induced by antigen vaccination in NOD mice. *Diabetes.* 2003;52:335–41.
94. Cahana A, Reiner O. LIS1 and platelet-activating factor acetylhydrolase (Ib) catalytic subunits, expression in the mouse oocyte and zygote. *FEBS Lett.* 1999;451:99–102.
95. Shyamasundar S, Jadhav SP, Bay BH, Tay SS, Kumar SD, Rangasamy D, Dheen ST. Analysis of epigenetic factors in mouse embryonic neural stem cells exposed to hyperglycemia. *PLoS One.* 2013;8:e65945.
96. Maerz S, Liu CH, Guo W, Zhu YZ. Anti-ischaemic effects of bilobalide on neonatal rat cardiomyocytes and the involvement of the platelet-activating factor receptor. *Biosci Rep.* 2011;31:439–47.

97. Overbergh L, Valckx D, Waer M, Mathieu C. Quantification of murine cytokine mRNAs using real time quantitative reverse transcriptase PCR. *Cytokine*. 1999;11:305–12.
98. Hasegawa S, Kohro Y, Shiratori M, Ishii S, Shimizu T, Tsuda M, Inoue K. Role of PAF receptor in proinflammatory cytokine expression in the dorsal root ganglion and tactile allodynia in a rodent model of neuropathic pain. *PLoS One*. 2010;5:e10467.
99. Yamada K, Hosokawa M, Yamada C, Watanabe R, Fujimoto S, Fujiwara H, Kunitomo M, Miura T, Kaneko T, Tsuda K, Seino Y, Inagaki N. Dietary corosolic acid ameliorates obesity and hepatic steatosis in KK-Ay mice. *Biol Pharm Bull*. 2008;31:651–5.
100. Kobayashi K, Imagama S, Ohgomori T, Hirano K, Uchimura K, Sakamoto K, Hirakawa A, Takeuchi H, Suzumura A, Ishiguro N, Kadomatsu K. Minocycline selectively inhibits M1 polarization of microglia. *Cell Death Dis*. 2013;4:e525.
101. Kigerl KA, Gensel JC, Ankeny DP, Alexander JK, Donnelly DJ, Popovich PG. Identification of two distinct macrophage subsets with divergent effects causing either neurotoxicity or regeneration in the injured mouse spinal cord. *J Neurosci*. 2009;29:13435–44.
102. Font-Nieves M, Sans-Fons MG, Gorina R, Bonfill-Teixidor E, Salas-Pédomo A, Márquez-Kisinousky L, Santalucia T, Planas AM. Induction of COX-2 enzyme and down-regulation of COX-1 expression by lipopolysaccharide (LPS) control prostaglandin E2 production in astrocytes. *J Biol Chem*. 2012;287:6454–68.
103. Pan J, Jin JL, Ge HM, Yin KL, Chen X, Han LJ, Chen Y, Qian L, Li XX, Xu Y. Malibatol A regulates microglia M1/M2 polarization in experimental stroke in a PPAR γ -dependent manner. *J Neuroinflammation*. 2015;12:51.

Submit your next manuscript to BioMed Central and we will help you at every step:

- We accept pre-submission inquiries
- Our selector tool helps you to find the most relevant journal
- We provide round the clock customer support
- Convenient online submission
- Thorough peer review
- Inclusion in PubMed and all major indexing services
- Maximum visibility for your research

Submit your manuscript at
www.biomedcentral.com/submit

